American Mineralogist, Volume 71, pages 472–500, 1986

Tourmaline as a recorder of pegmatite evolution: Bob Ingersoll pegmatite, Black Hills, South Dakota

Bradley L. Jolliff, James J. Papike, Charles K. Shearer
Institute for the Study of Mineral Deposits, South Dakota School of Mines and Technology, Rapid City, South Dakota 57701-3995

Abstract

Tourmaline occurs as an accessory mineral in five of six zones in the Li-, B-, Be-, Nb-, Ta-, and Sn-enriched, internally zoned Bob Ingersoll No. 1 pegmatite located in the Precambrian core of the southern Black Hills near Keystone, South Dakota. The purpose of this investigation is (1) to examine the usefulness of tourmaline as a petrogenetic indicator in this setting and (2) to apply this indicator to interpret the internal evolution of the pegmatite. Tourmaline occurs in ten distinct types based on texture or habit and coexisting mineral assemblage. Chemical analyses of the tourmaline show compositional differences between types that may be useful in determining the crystallization sequence and differentiation mechanisms. Trends of major-element variations in tourmaline from the country rock to the core include the following: (1) Mg and Ti decrease abruptly from the country rock through the border zone to the wall zone; (2) Fe decreases and (Li + Al) increase from the wall zone to the core; and the minor elements Mn, Zn, and Ca generally increase toward the core. Tourmaline compositional trends in this pegmatite, coupled with textural features and mineral associations, provide evidence of an inward, generally sequential crystallization of the border zone, wall zone, intermediate zones, and finally the core, but with overlap between the inner wall zone and intermediate zones. The pegmatite melt was probably saturated at the onset of crystallization; however, fluid exsolution may have temporarily stopped during the initial crystallization of the third intermediate zone and a period of tourmaline instability, but then resumed, along with tourmaline crystallization, during the formation of the pegmatite core.

Introduction

Tourmaline is a common accessory mineral in pegmatites that surround the Harney Peak Granite at the core of the Precambrian terrane of the southern Black Hills. This area is a classic example of a pegmatite field surrounding a granitic intrusion that may belong to the same magmatic system (Redden et al., 1982). The pegmatites consist predominantly of small, layered, and weakly zoned dikes, but include a number of large, internally zoned, rare-element pegmatite bodies. Pegmatitic rocks in general have been the subject of a tremendous quantity of research and geologic literature (e.g., Jahns, 1955), and the Black Hills pegmatites have also been extensively studied (Page and others, 1953; Sheridan et al., 1957; Norton et al., 1962; Redden, 1963). A detailed model of the crystallization of pegmatite was presented by Jahns and Burnham (1969) and was recently summarized by Jahns (1982). Although great progress has been made in pegmatite research, many questions remain regarding the internal evolution of zoned pegmatite bodies (e.g., Černý, 1975, 1982; Jahns, 1982).

The study of zoned pegmatites by classical petrologic methods such as whole-rock chemical analysis is hampered by the coarse grain size of minerals, by the heterogeneity of large sections of the pegmatite, and by poor exposure in three dimensions. In addition, much of the volume of well-exposed zoned pegmatites has been mined or eroded; therefore, bulk compositions may only be estimated. One approach that may overcome such difficulties is the use of minerals with variable compositions as recorders of petrogenetic information (e.g., Foord, 1976; Shearer et al., 1985).

Tourmaline occurs in many of the pegmatites surrounding the Harney Peak Granite, in the granite itself, and in the country rock of contact zones surrounding both granite and pegmatite. The crystal structure of tourmaline is such that it allows substitution of a variety of ions with respect to both size and charge. Additionally, tourmaline is the dominant boron-bearing mineral and is the dominant mafic silicate in many of the zoned pegmatites of the Black Hills. These properties make tourmaline potentially well suited for the detailed study of chemical variation within a pegmatite during its internal evolution. The purpose of this study is to characterize the compositional and textural variations of tourmaline in a large, internally zoned pegmatite and to evaluate the use of tourmaline in this setting as a recorder of crystallization history. Compositional and textural trends of tourmaline are then applied toward interpretation of the internal evolution of the Bob Ingersoll pegmatite.

The idea of using the chemical variability of tourmaline to decipher petrogenetic details is not unique to this study.

0003–004X/86/0304–0472$02.00

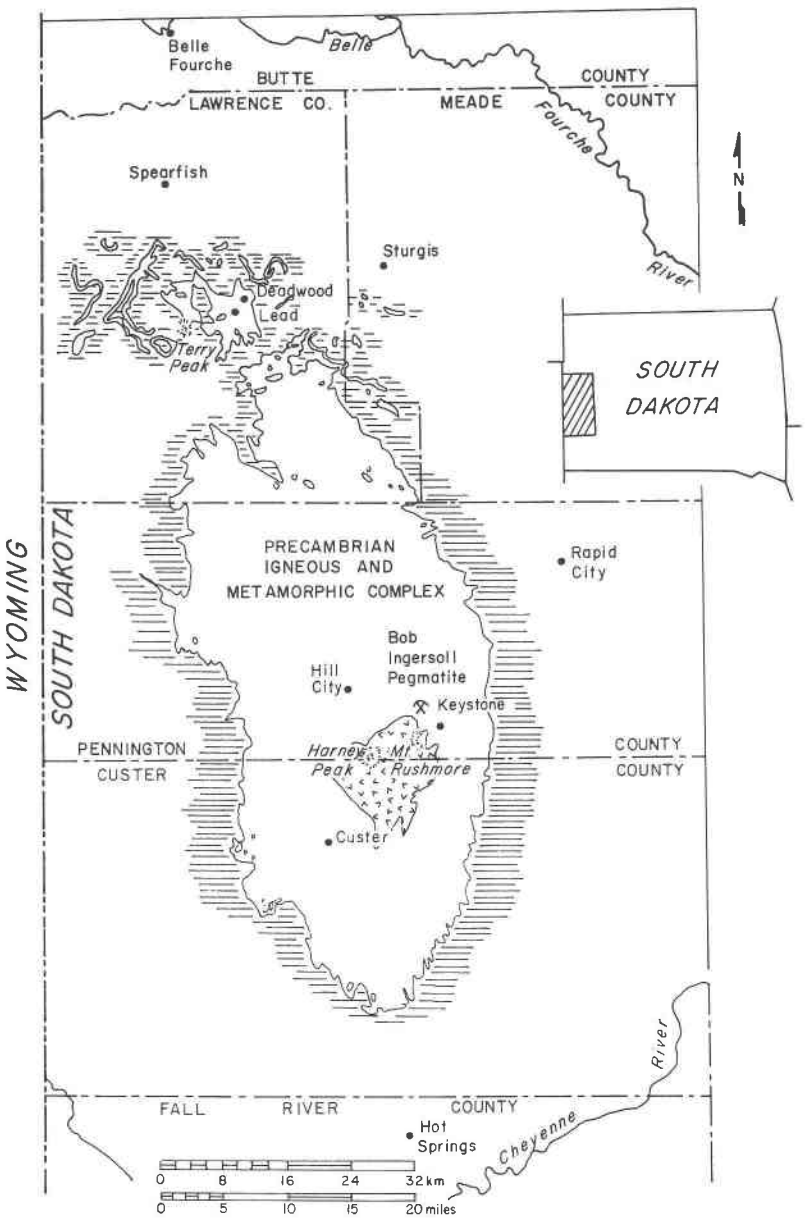

Fig. 1. Location of the Bob Ingersoll pegmatite in the Precambrian core of the Black Hills. Harney Peak Granite shown by random V pattern.

It has long been known that the color and other optical properties of tourmaline are roughly indicative of its chemistry (Jenks, 1935; Carobbi and Pieruccini, 1947; Bradley and Bradley, 1953; El-Hinnawi and Hofmann, 1966; Leckebusch, 1978; Rose et al., 1981) and that these properties may be used to indicate the fractionation trends and relative degree of evolution of the rocks that host the tourmaline. Staatz et al. (1955) established systematic compositional variation trends in tourmaline, from the wall inward, of the bizonal Brown Derby pegmatite dikes of the Quartz Creek district of Gunnison County, Colorado. They found the major variation from the outer wall zone to the core to be an increase of Li concomitant with a decrease of Fe. Foord (1976, 1977) characterized the compositional variation of tourmaline in layered, miarolitic pegmatite dikes and host rocks of the Himalaya pegmatite-aplite dike system in San Diego County, California. These and other studies (Power, 1968; Neiva, 1974; Manning, 1982; Henry and Guidotti, 1985) have shown tourmaline to exhibit systematic compositional variations and to be an effective recorder of petrogenetic information.

The pegmatite selected for study is the Bob Ingersoll No. 1 dike, located 2 mi (3.2 km) northwest of Keystone, in Pennington County, South Dakota, near the northern border of NW1/4 Sec. 6, T2S, R6E (Fig. 1). The Bob

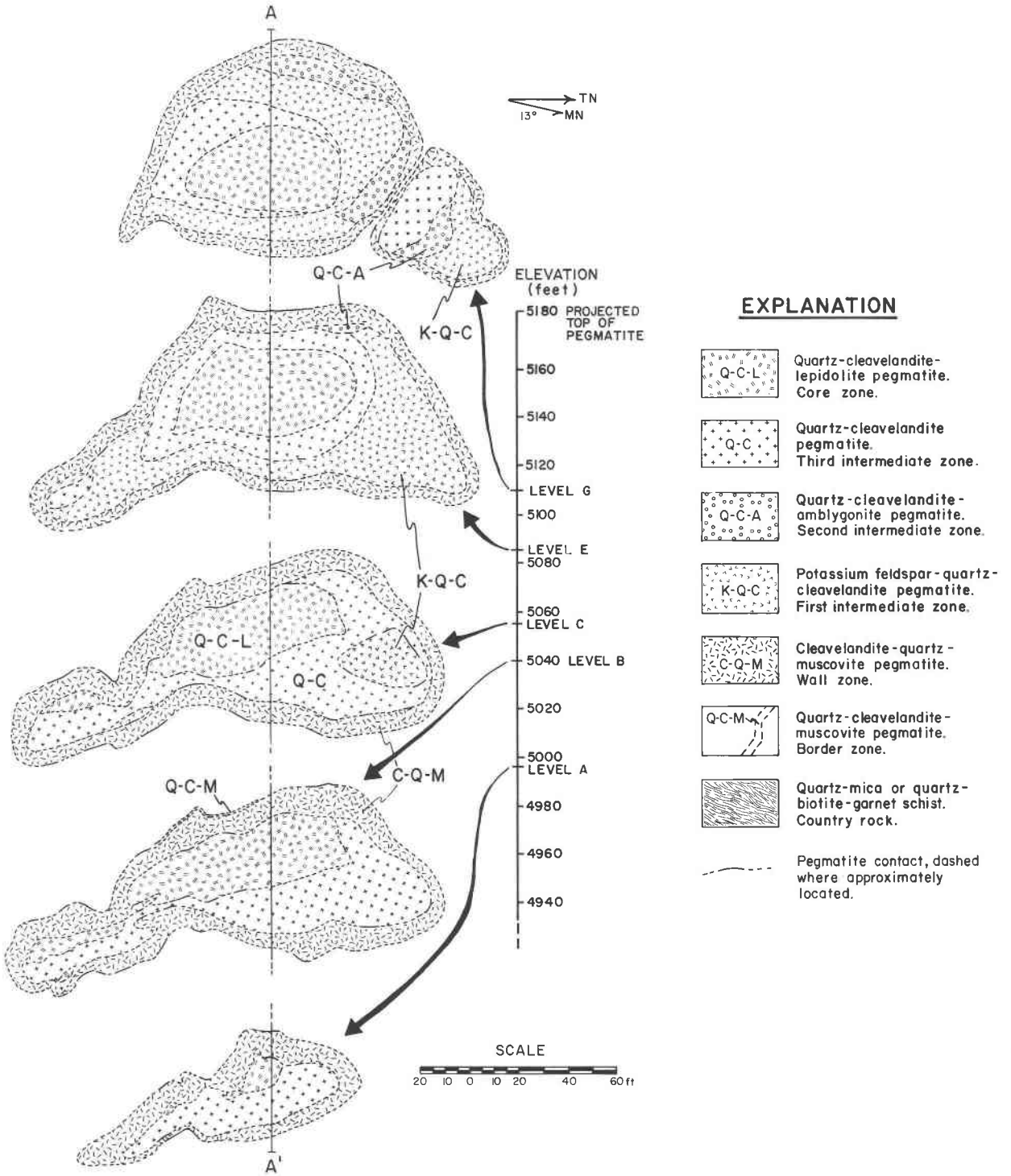

Fig. 2. Horizontal geologic sections of Bob Ingersoll No. 1 dike showing distribution of pegmatite zones. Geology based on mapping as part of this work and mapping by Hanley (1953) in areas now mined out, backfilled, or flooded.

Ingersoll No. 1 dike is a large, zoned B-, Be-, Nb-, Ta-, Sn-, and Li-enriched pegmatite that contains tourmaline as an accessory mineral in five of the six zones. This pegmatite was selected because of the abundance and variability of the tourmaline, the good surface and underground exposures, and because it was mapped and described during an earlier stage of its mining history (Hanley, 1953; in Page and others). As part of the present work, the pegmatite was remapped to include new exposures and to establish precise locations of samples. Tourmalines

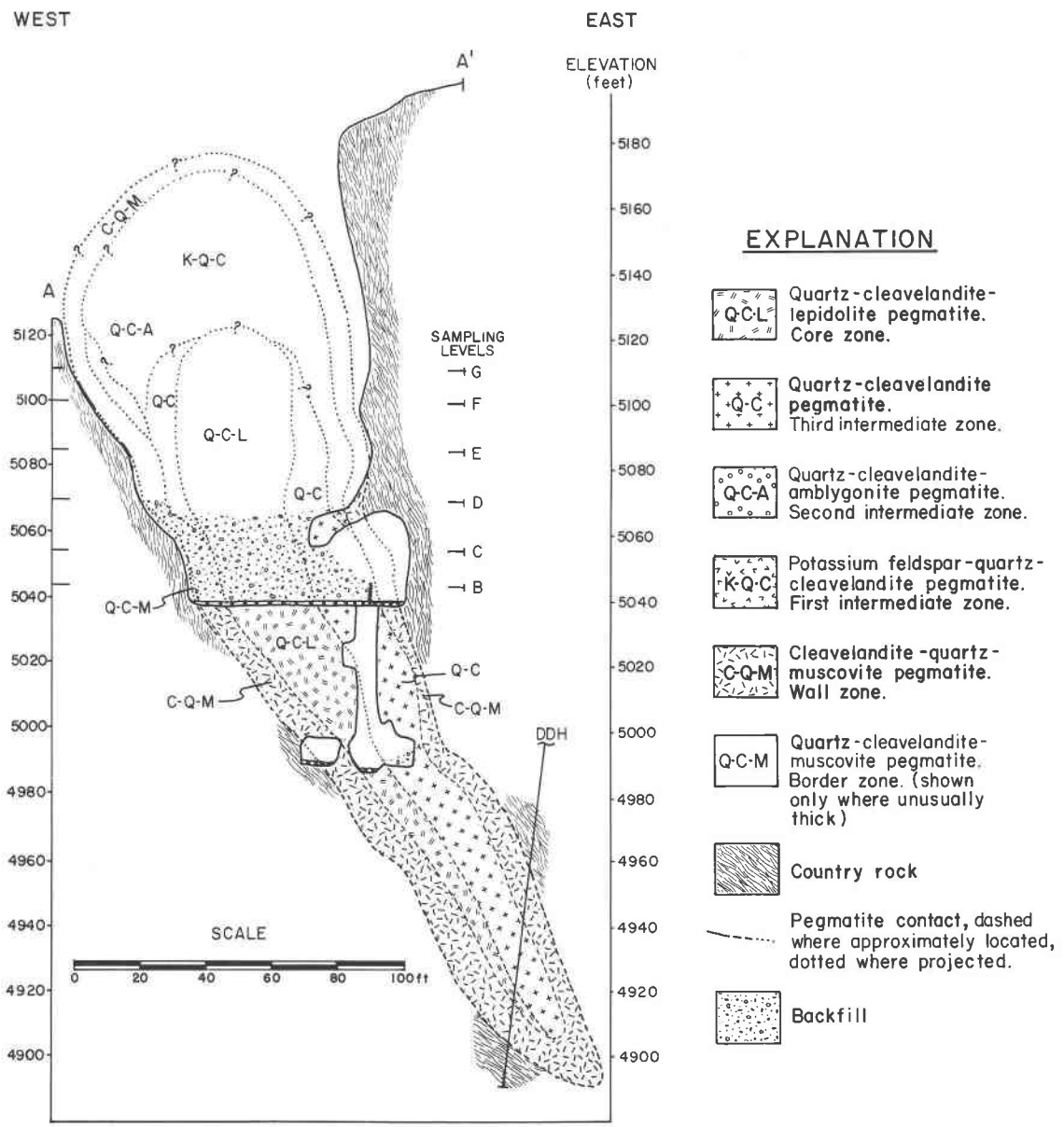

Fig. 3. Cross section A–A′ of Bob Ingersoll No. 1 dike. Geology below 5040-ft (1536-m) level based on Hanley (1953). Distribution of zones in area of above-surface projection based upon exposures north and south of section line.

from 45 sample locations have been analyzed using microprobe, neutron activation, and atomic absorption techniques.

Tourmaline occurs in ten distinct associations at the Bob Ingersoll No. 1 dike. Descriptions of the textural types and an overview of the geology of the pegmatite dike are given in the next section.

Several of the important questions addressed by this study are as follows: (1) Does tourmaline show consistent, systematic compositional variations related to spatial distribution in the pegmatite, e.g., vertical position or zonal location? (2) Do textural variations of tourmaline correspond to compositional variations? (3) Do the compositional variations indicate the sequence of crystallization of the pegmatite zones? Is the sequence consistent with mineral assemblages and textures? (4) Do compositional and textural variations of tourmaline reflect changes in the crystallization process and the nature of the crystallizing medium?

Geology of Bob Ingersoll No. 1 dike

The No. 1 dike was mined extensively between 1922 and 1945, principally for lepidolite, beryl, and amblygonite. Since the time of previous mapping, several subsurface levels have been flooded, and additional mining has exposed new surfaces. As part of this study, the No. 1 dike was remapped by plane-table surveying of

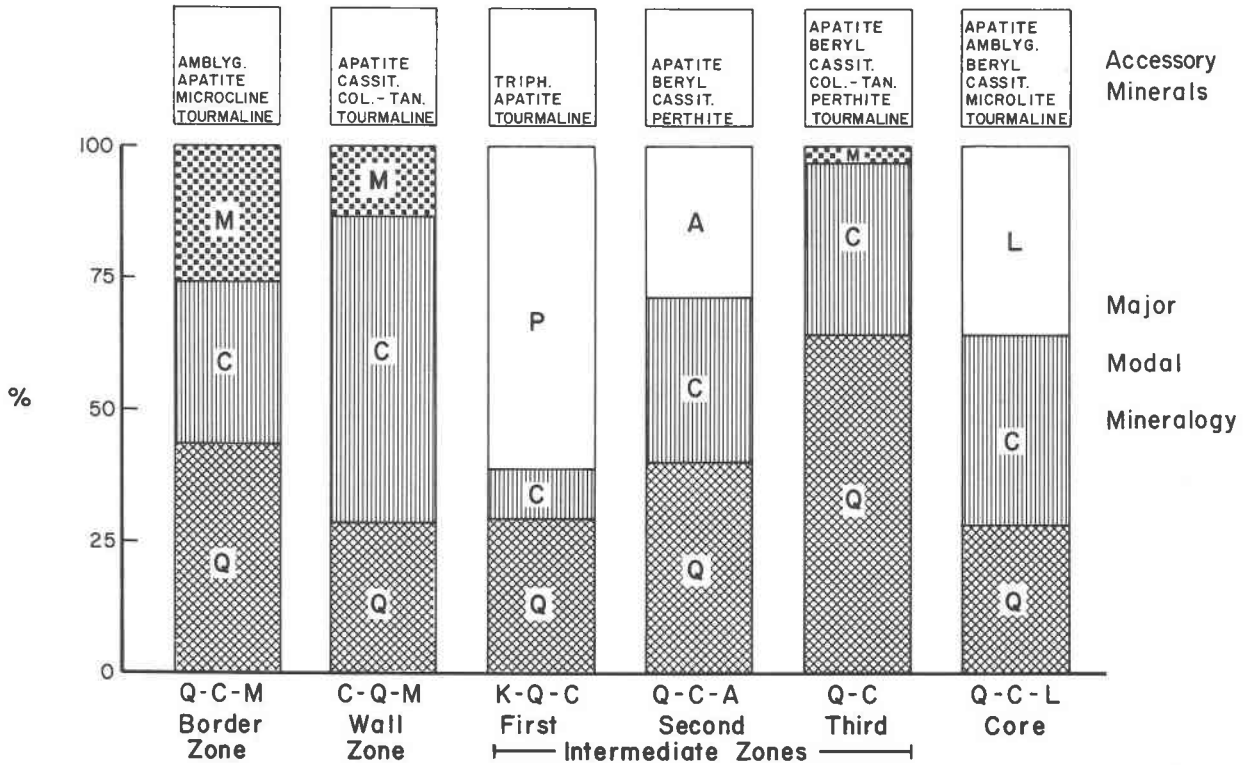

Fig. 4. Approximate average modal composition of pegmatite zones. Symbols: Q, quartz; C, cleavelandite; M, muscovite; P, perthite; A, amblygonite-montebrasite; L, lepidolite. Abbreviations: Cassit, cassiterite; Amblyg, amblygonite-montebrasite; Col-Tan, columbite-tantalite; Triph, triphylite-lithiophilite.

successive levels of the pegmatite. The structure of the dike is shown as a series of horizontal sections in Figure 2.

The No. 1 dike is an inclined and flattened funnel-shaped pegmatite, approximately 25 × 30 m in plan near the top, and is at least 75 m deep (Fig. 3). The long axis of the dike trends north-northwest, and the deep root of the dike plunges to the southeast.

The pegmatite of the No. 1 dike conformably intrudes metamorphic rocks consisting predominantly of biotite-garnet-staurolite schist and minor quartzite. The pegmatite–country rock contact is sharp and easily recognized, but locally irregular in shape. The contact is generally paralleled by schistosity in the country rock. The conformable nature of the schistosity around the dike in general, and where the contact bulges or rolls, suggests a relatively ductile country-rock response as it was shouldered aside by the intruding pegmatite.

The dike is shown in vertical cross section in Figure 3. Much of the upper portion of the dike has been mined; however, the structure of the central portion as it existed prior to mining can be broadly inferred from exposures within and around the perimeter of the glory hole.

Zones

There are six pegmatite zones in the No. 1 dike, distinguishable by their texture or mineralogy. These include a border zone, wall zone, three intermediate zones, and the core. Approximate average modes for each of the zones are given in Figure 4. Modes are based on visual estimates and grid counts (10-cm spacing) of present exposures with consideration given to abundances expressed by Hanley (1953).

The border zone is generally very fine grained (see grain size scheme, Table 1) and consists of varying proportions of quartz, albite (or cleavelandite), and muscovite. Microcline, present in small quantities, is surrounded by reaction rims of muscovite. Several accessory minerals are present, including tourmaline, apatite, and amblygonite. Tourmaline is commonly the coarsest mineral in the border zone, attaining lengths up to 2.5 cm. Tourmaline occurs as slender, tapered crystals that are oriented subperpendicular to the contact with country rock, with the tapered end nearest to the contact. Some of the crystals are inclined or nearly parallel to the contact, a feature that may represent flow alignment or may indicate the presence of inclined gradients caused by the flowage of melt interior to the border zone as it crystallized. The border zone is nearly continuous around the pegmatite and ranges in thickness from 1 to 10 cm. The transition from border to wall zone is sharp, commonly occurring over a distance on the order of centimeters, and is marked by an abrupt increase in grain size.

The wall zone characteristically contains the assemblage cleavelandite-quartz-muscovite. Cleavelandite is generally most abundant and is typically intergrown with quartz or in virtually monomineralic aggregates as much as 1 × 1 m in cross section. Muscovite is generally medium to coarse grained and occurs as isolated books as much as 30 cm in long dimension. Slender prismatic tourmaline is intergrown with the coarse muscovite, and very coarse tourmaline occurs with the large cleavelandite aggregates. Fine- to medium-grained rocks also occur in the wall zone, but are more common in the footwall exposures. A notable trend in the major modal mineralogy of the wall zone is a decrease in the abundance of cleavelandite and an increase in the abun-

dance of quartz from the outer part of the wall zone toward the interior. The wall zone, which forms a continuous unit around the pegmatite, ranges in thickness from 1 to 3 m. It is commonly thickest on the footwall portion of the zone. Depending upon position in the dike, the wall zone contacts each of the intermediate zones, which are discontinuous (Figs. 2, 3). These contacts, which are gradational, were mapped close to the appearance of the mineral that characterizes the zone (e.g., potassium feldspar, first intermediate; amblygonite-montebrasite, second intermediate, etc.).

The first intermediate zone is distinguished by the presence of coarse-grained to very coarse grained potassium feldspar crystals that are set in a matrix consisting largely of massive quartz and smaller amounts of cleavelandite. Muscovite is present in small quantity particularly where this zone contacts the wall zone. The abundance of potassium feldspar and its grain size decrease toward contacts with other zones. In the pinnacle of the glory hole, now mined out, which was spatially close to the middle of the zone, perthite was reported to compose 90% of the rock (Hanley, 1953). Single feldspar crystals currently exposed in the mine are as much as 3 m across in the maximum exposed dimension.

The second intermediate zone is distinguished by the abundance of amblygonite-montebrasite ($Amb_{25}Mbs_{75}$). This zone is discontinuous and occurs in what are inferred to be irregular lens-shaped units between the first intermediate zone and the core, third intermediate zone, or wall zone. Amblygonite-montebrasite forms as circular masses as much as 2 m in diameter. This zone appears to be confined to the upper 25 to 30 m of the dike, although amblygonite-montebrasite occurs in trace quantities in other zones lower in the dike.

The third intermediate zone is composed predominantly of medium-grained to very coarse grained quartz intergrown with cleavelandite that forms as discrete grains as well as in a veinlike mosaic pattern between quartz grains. The general texture of this zone is similar to the texture of the quartz and cleavelandite matrix of the first and second intermediate zones. This zone is more continuous than the first or second intermediate zones and almost entirely surrounds the core. It is discontinuous along the footwall in lower parts of the dike where the core abuts the wall zone. In the central and lower parts of the dike, where the first and second intermediate zones are absent, the third intermediate zone directly contacts the wall zone. An accessory mineral assemblage of tourmaline, beryl, apatite, and cassiterite typically occurs at contacts between the third intermediate zone and the core.

The core of the pegmatite contains principally quartz, cleavelandite, and lepidolite (3.5 to 6.0 wt% Li_2O in lepidolite). Quartz and cleavelandite are fine to medium grained, but cleavelandite also occurs in large pod-shaped aggregates. Lepidolite is very fine grained, and in several exposures large aggregates are composed almost entirely of lepidolite. The lepidolite content appears to increase from outer contacts of the core inward.

Tourmaline occurrences and textures

The various occurrences of tourmaline at the Bob Ingersoll No. 1 dike can be grouped according to their texture or habit, color, and mineral association. (Groups are hereafter referred to as types.) Each type tends to occur characteristically in a given zone. Ten types have been identified (including tourmaline in the country rock); their distinguishing characteristics and zonal distribution in the pegmatite are summarized in Table 1.

Country rock adjacent to contacts with pegmatite is extensively tourmalinized (Tuzinski, 1983; Shearer et al., 1986). In samples of country rock from outside the pegmatite, dark-brown tourmaline (type 1a) partially replaces biotite, whereas ferromagnesian components of country-rock inclusions within the pegmatite are completely tourmalinized (type 1b). Fine-grained, dark-green tourmaline (type 2) occurs in the border zone as euhedral, slender, tapered prisms. These crystals are commonly fractured perpendicular to the c axis, and the fractures are filled by the fine-grained matrix characteristic of the zone.

Table 1. Tourmaline distribution at the Bob Ingersoll No. 1 dike

Occurrence		Color*	Texture	Grain size**	Type
Country rock & country rock inclusion		Dark brown to black	Poikiloblastic, sub- to euhedral, short prismatic	vf-f	1a 1b
Pegmatite Zones					
Border zone		Dark green	Tapered, slender prismatic	vf-f	2
Wall zone	(1)	Black to dark blue	Euhedral, tapered, prismatic to massive splays	m-vc	3
	(2)	Medium Blue	Subhedral, in allotriomorphic-granular matrix	f-m	4
	(3)	Blue-green	Euhedral, intergrown with coarse muscovite	f-m	5
	(4)	Green	Anhedral, comprises small veinlets	f	6
First intermediate zone		Dark blue to green	Subhedral, intergrown with quartz, cleavelandite	f-m	7
Third intermediate zone		Green to light green	Anhedral to euhedral, short prismatic, intergrown with quartz-cleavelandite-beryl-apatite	m	8
Core	(1)	Light blue to grey	Anhedral to subhedral, intergrown with fine-grained quartz-cleavelandite-lepidolite	f-m	9
	(2)	Pink to red	Sub- to euhedral, commonly splayed, and intergrown with quartz	f-m	10

Notes:
* Macroscopic color
** Grain size scheme:
vf - very fine - <6 mm
f - fine - 6 mm to 2.5 cm
m - medium - 2.5 cm to 10 cm
c - coarse - 10 cm to 30 cm
vc - very coarse - >30 cm

Black tourmaline occurs in the wall zone near the border zone contact. This tourmaline (type 3) is generally coarse to very coarse grained ranging up to 1.5 m in length, but may also be fine or medium grained, and may occur within inches of the border zone. Away from the border zone, toward the inner contact of the wall zone, the color of the tourmaline is dark blue. The very coarse tourmaline is oriented with the c axis perpendicular to, and tapered toward, the outer contact of the pegmatite. Small branches of tourmaline splay from the main body of individual crystals, clearly indicating the direction of growth (Fig. 5a). These crystals are generally euhedral and are not embayed by other minerals, although they can contain fracture fillings.

Fine-grained, medium-blue, subhedral tourmaline forms a second texturally distinct type in the wall zone (type 4). Such crystals occur in interior parts of the wall zone as intergrowths with fine-grained aggregates of cleavelandite, quartz, and muscovite.

A very distinctive bimineralic assemblage of tourmaline epitaxially intergrown with coarse muscovite also occurs in the wall zone (type 5). The tourmaline is generally euhedral, forming fine-

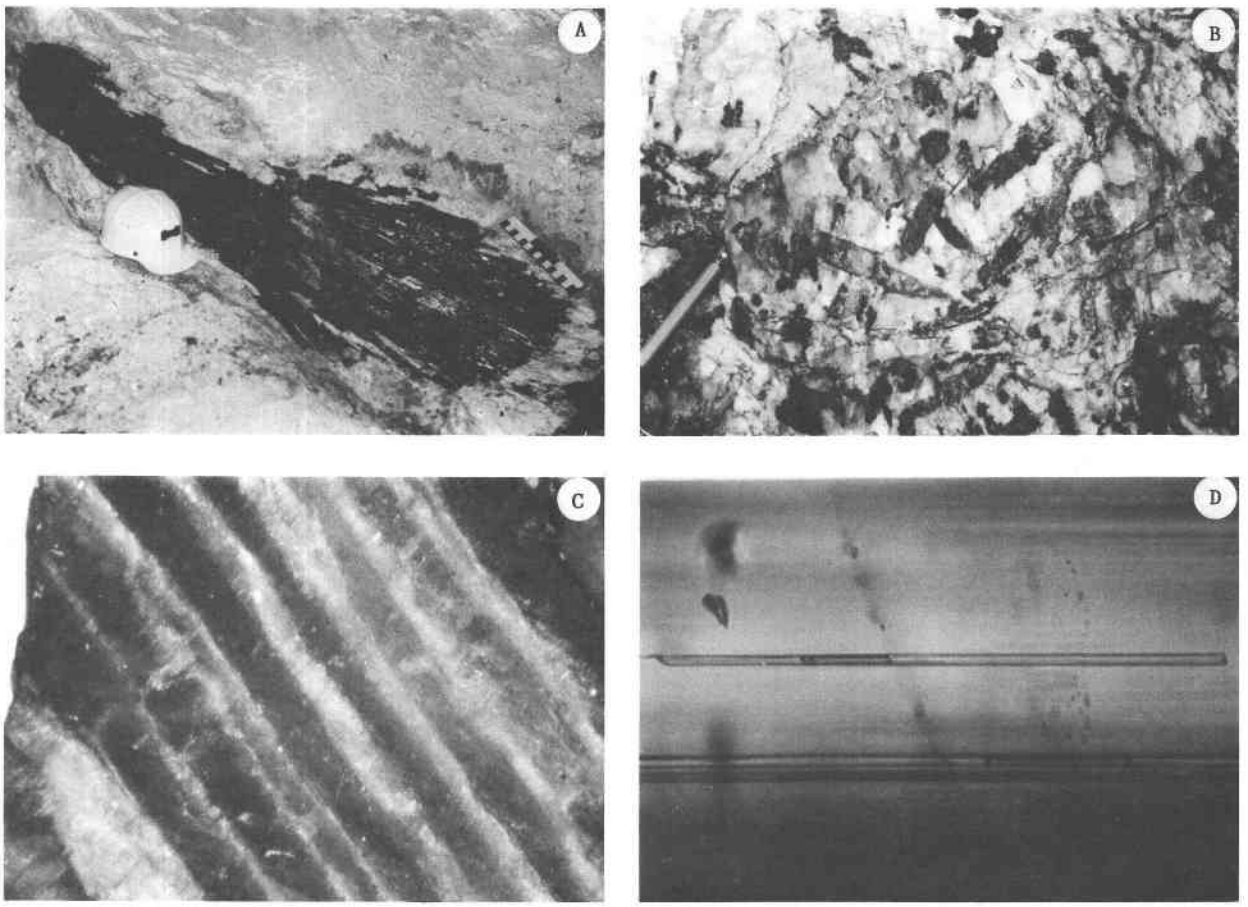

Fig. 5. (A) Type 3 tourmaline from the wall zone. White mineral encasing tourmaline is cleavelandite (sample B7). (B) Type 8 tourmaline from third intermediate zone adjacent to contact with core. Note pen for scale (sample B11). (C) Photomicrograph of texture resembling exsolution. Dark bands are Fe-rich; light bands are Fe-depleted. Width of photo is 4 mm (reflected light, crossed polars). (D) Elongate fluid inclusions parallel to c axis, which impart chatoyancy to the light bands shown in C. Length of centered inclusion is approximately 50 μm.

to medium-grained, slender prisms. Some of these are finely color-zoned, with dark-blue cores, light-blue and green intermediate zones, and colorless rims.

Green tourmaline occurs as thin (<1 cm) fracture fillings in the wall zone (type 6). This type has been found only in cross-cutting relationships with very coarse, type 3 tourmaline. Such tourmaline veins extend no more than several centimeters into the surrounding rock from the tourmaline that they transect.

Tourmaline is not an abundant accessory mineral in the first intermediate zone. Its occurrence is limited to bluish-green, subhedral to anhedral crystals that are fine grained or form fine- to medium-grained aggregates (type 7). Tourmaline aggregates are intergrown with the quartz-cleavelandite matrix of this zone.

In the third intermediate zone, tourmaline is characteristically medium to light green (type 8). The typical habit is one of medium-grained, stubby prismatic crystals (Fig. 5b). In several cases, euhedral tourmaline forms skeletal crystals, cores of which consist of the assemblage quartz, apatite, and beryl. This texture probably formed by early nucleation and growth of euhedral tourmaline, followed by cocrystallization with quartz, beryl, and apatite, which commonly filled in the open end of the tapered tourmaline crystals (Norton et al., 1962). Green tourmaline of this zone is also found as anhedral grains around the rims of coarse, pillow-shaped aggregates of radially grown cleavelandite laths.

Tourmaline in the pegmatite core consists of two texturally distinct varieties. Very light blue, fine-grained, poikilitic subhedral tourmaline is intergrown with fine-grained aggregates of quartz, cleavelandite, and lepidolite. Pink, euhedral tourmaline (elbaite) also occurs in the core, but appears to be associated with small quartz segregations, although it also occurs in quartz-cleavelandite-lepidolite aggregates.

Analytical procedures

Tourmaline was collected from 45 sample locations, chosen to represent the entire range of textural types present at the pegmatite (see Table 2). For those types showing a broad range of compositions after initial analyses, additional samples were taken to characterize the full compositional range (types 2, 3, and 5). Sampling is biased toward the wall zone owing to the abundance of tourmaline in the wall zone versus interior zones and to the volume of the zones currently available for sampling. Most of the volume of zones containing types 7, 8, 9, and 10 tourmaline has been mined from the pegmatite.

Tourmaline grains were analyzed for ten major and minor elements by microprobe techniques using the fully automated MAC electron microprobe at the South Dakota School of Mines and Technology. The wavelength-dispersive system with TAP, PET, and LIF crystals, was utilized for quantitative determinations of Si, Ti, Al, Fe, Mg, Mn, Zn, Ca, Na, and K. All analyses were conducted at an accelerating voltage of 15 kV, a beam current of approximately 0.0150 μA, and a counting time of 20 000 counts or 20 s. Corrections were made with the empirical correction technique of Bence and Albee (1968). A minimum of five analyses were taken per grain; however, as many as 20 analyses were taken to characterize zoned grains.

Tourmaline separates were prepared for 27 samples, using a combination of hand picking, magnetic separation, and heavy-liquid separation. Ferrous iron determinations were conducted using standard $KMnO_4$ titration, following HF-H_2SO_4 dissolution in pressurized Teflon-lined Paar bombs. The separates were also used for lithium and trace-element determinations by atomic absorption spectrometry. Fluorine contents were determined by ion selective electrode (Bodkin, 1977). Data for 15 major, minor, and trace elements were obtained by INAA using a high efficiency 130-cm^3 Ge(Li) detector (25% FWHM 108 keVγ of ^{60}Co), a 4096 channel analyzer and coincidence-noncoincidence Ge(Li)-NaI(Tl) counting systems at the Battelle Pacific Northwest Laboratories. The details of the INAA procedure and the systematics of coincidence-noncoincidence counting are described by Laul (1979).

Thirteen samples that span the range of compositions were analyzed by X-ray powder diffraction to determine unit-cell parameters. The study was conducted with a Norelco diffractometer mounted on a Philips constant potential generator, equipped with a graphite crystal monochromator, θ-compensator, and sample spinner. Experimental conditions included Cu$K\alpha$ radiation, 40 kV, 20 mA, ½° per minute scan speed, and an Al_2O_3 internal standard.

Table 2. Tourmaline sample population

Tourmaline type	Sample locations	Grains analyzed by microprobe	Microprobe analyses
1a	2	5	12
1b	3	6	23
2	3	12	59
3	10	25	155
4	4	7	32
5	7	12	62
6	1	6	49
7	3	4	21
8	4	5	26
9	2	3	16
10	1	2	22

Results

Results of chemical analyses of the suite of 27 samples are presented in Table 3. Cations per formula unit were calculated based on normalization to six silicons (see also Fortier and Donnay, 1975; Sahama et al., 1979; Walenta and Dunn, 1979). The reason for this normalization is that Si is consistently determined to be slightly in excess of six atoms per formula unit when normalized against oxygen for charge-balance. Such excesses, although usually small (less than 0.05 atoms per formula unit), are difficult to reconcile in terms of the structure of tourmaline (next section).

The danger of conducting analyses on powders taken from whole or multiple crystals that are compositionally heterogeneous or zoned is well known (e.g., Donnay, 1968; Foord, 1976). The values presented in Table 3 are average analyses; however, several of the samples are compositionally zoned and are therefore difficult to characterize in terms of Li content, which must be determined from chemical analyses of powders. Li contents determined for nonzoned tourmaline, however, correlate well (inversely) with Fe contents (correlation coefficient $\simeq -0.95$). The Fe contents determined by microprobe anlysis were used to approximate the Li contents of zoned samples.

Total Fe determined by microprobe analysis is reported as FeO. Many ferrous iron determinations indicate that a high percentage of the total Fe is ferrous; however, due to variable oxidation during dissolution, the results are not reproducible. The good correlation of Fe and Li values also indicates that a high percentage of the total Fe is ferrous. The green color of some of the tourmaline (types 2, 5, 6, 7, 8) may indicate the presence of Fe^{3+}, in combination with Fe^{2+}, as a chromophore (Taylor and Terrell, 1967; Wilkins et al., 1969; Moore, 1982). Green color may, however, also result from Fe^{2+}-Ti^{4+} charge-transfer processes (Faye et al., 1974).

Results of the unit-cell determinations are listed in Table 4 and values of a and c are plotted in Figure 6. The cell parameters correspond closely with the compositions listed in Table 3. All samples plot close to the schorl-elbaite reference line (Donnay and Barton, 1972). Samples with detectable MgO are displaced slightly toward higher values of c.

Compositions of zoned crystals

Tourmaline crystals of types 1, 2, 3, and 5 are typically zoned (Figs. 7, 8). Crystals of tourmaline in the country rock (types 1a and b) contain cores with low values of Fe/(Fe + Mg) (e.g., 0.54 to 0.67) relative to rims (0.68 to 0.80). Type 1a tourmaline, near the pegmatite contact, replaces biotite that has Fe/(Fe + Mg) values of approximately 0.73. Farther out from the pegmatite (20 m), the Fe/(Fe + Mg) value of biotite decreases to 0.61. The Fe/(Fe + Mg) values of tourmaline in the country rock approach, but do not overlap appreciably, the Fe/(Fe + Mg) values of tourmaline in the border zone (Fig. 9).

Individual crystals of the border zone (type 2) contain high Mg and Fe in their cores relative to their rims (Fig. 7a), and Fe/(Fe + Mg) values lower in the cores than in the rims. Crystals with two repetitions of this type of zoning also occur (Fig. 8). Zn, Mn, and Ca are in general inversely correlative with Ti, Mg, and Fe. In the wall zone, type 3 tourmaline is zoned with high Fe at the tapered end, nearest the outer contact of the wall zone, and low Fe on the growth surfaces toward the interior of the zone (Figs. 7b, 7c). Crystals of tourmaline intergrown with muscovite in the wall zone (type 5) are strongly zoned concentrically about the c axis, but not as much along their length. This zonal arrangement and the shape of the crystals reflect the favorability of growth in the c direction.

Table 3. Average analyses of representative samples from each of the textural types (indicated in parentheses) of tourmaline at the Bob Ingersoll No. 1 dike

Zone	Country rock (1a)	(1b)	Border zone (2)	Wall zone type 3 Outer wall zone									Inner wall zone	Wall zone fracture filling (6)
Sample	C'11	B7c	B2	B3	E1a2	C'1	B7a	B7b	B6b	B6c	B6a	C'4a	C'4b	D1	B7(1)
SiO_2	35.61	34.80	36.28	35.40	35.68	35.26	35.66	36.32	36.38	36.43	36.45	36.43	36.70	36.09	37.35
TiO_2	0.93	0.65	0.12	0.05	0.05	0.03	nd	0.08	nd	nd	0.09	nd	nd	nd	0.05
Al_2O_3	31.60	31.44	35.91	33.58	34.40	34.14	34.70	34.85	35.33	35.36	36.86	35.40	35.97	36.25	36.46
FeO*	9.88	8.55	6.21	11.71	11.58	10.71	9.64	9.14	6.79	6.67	6.21	6.11	6.50	5.85	5.69
MgO	2.76	1.95	0.84	0.08****	0.07	0.03	0.02	0.03	0.01	0.01	<0.01	0.01	0.01	0.01	0.03
MnO	0.13	0.11	0.33	0.26	0.25	0.30	0.30	0.18	0.30	0.43	0.47	0.51	0.34	0.66	0.30
ZnO	0.10	0.44	0.34	0.70	0.75	0.90	0.85	0.84	1.27	1.35	1.72	1.57	1.63	1.69	0.76
CaO	0.05	0.03	0.11	0.04	0.05	0.04	0.05	0.04	0.06	0.06	0.05	0.07	0.09	0.09	0.13
Na_2O	2.34	2.32	2.53	1.91	1.75	2.13	2.04	2.34	2.44	2.45	2.08	2.48	2.38	2.29	2.40
K_2O	0.04	0.02	0.11	0.02	0.04	0.01	0.02	0.02	0.02	0.03	nd	0.01	0.03	0.02	0.02
Li_2O	0.67	0.47	0.96	0.41	0.50	0.61	0.71	0.65	1.08	1.13	1.05	1.13	1.18	1.13	1.48
F	1.12	1.26	1.39	0.81	0.91	0.93	1.08	1.05	1.37	1.43	1.42	1.41	1.36	1.37	1.48
Total	**85.23**	**82.04**	**85.13**	**84.97**	**86.03**	**85.09**	**85.07**	**85.54**	**85.05**	**85.35**	**86.40**	**85.13**	**86.19**	**85.44**	**86.15**
Cations per formula unit															
Si**	6.000	6.000	6.000	6.000	6.000	6.000	6.000	6.000	6.000	6.000	6.000	6.000	6.000	6.000	6.000
B***	3.000	3.000	3.000	3.000	3.000	3.000	3.000	3.000	3.000	3.000	3.000	3.000	3.000	3.000	3.000
Al (Z)	6.000	6.000	6.000	6.000	6.000	6.000	6.000	6.000	6.000	6.000	6.000	6.000	6.000	6.000	6.000
Al (Y)	0.275	0.389	1.000	0.708	0.818	0.847	0.881	0.785	0.867	0.864	1.151	0.872	0.931	1.103	0.903
Ti	0.118	0.084	0.015	0.006	0.006	0.004	--	0.010	--	--	0.011	--	--	--	0.006
Fe	1.392	1.233	0.859	1.660	1.629	1.524	1.356	1.263	0.937	0.919	0.855	0.842	0.889	0.813	0.764
Mg	0.693	0.501	0.207	0.020	0.017	0.008	0.005	0.007	0.002	0.003	0.001	0.002	0.002	0.001	0.007
Mn	0.019	0.016	0.046	0.037	0.036	0.043	0.043	0.025	0.042	0.060	0.066	0.071	0.047	0.093	0.041
Zn	0.012	0.056	0.042	0.088	0.093	0.113	0.106	0.102	0.155	0.164	0.209	0.191	0.197	0.207	0.090
Li	0.454	0.327	0.639	0.279	0.338	0.417	0.480	0.432	0.716	0.748	0.695	0.748	0.776	0.755	0.956
ΣY site	**2.963**	**2.606**	**2.808**	**2.798**	**2.937**	**2.956**	**2.871**	**2.624**	**2.719**	**2.758**	**2.988**	**2.725**	**2.842**	**2.972**	**2.767**
Ca	0.009	0.006	0.020	0.007	0.009	0.007	0.009	0.007	0.010	0.011	0.009	0.012	0.016	0.016	0.022
Na	0.764	0.776	0.811	0.628	0.571	0.703	0.666	0.749	0.780	0.782	0.664	0.792	0.754	0.738	0.748
K	0.009	0.004	0.023	0.004	0.009	0.002	0.004	0.004	0.004	0.006	--	0.002	0.006	0.004	0.004
ΣX site	**0.782**	**0.786**	**0.854**	**0.639**	**0.589**	**0.712**	**0.679**	**0.760**	**0.794**	**0.799**	**0.673**	**0.806**	**0.776**	**0.758**	**0.774**
F	0.597	0.687	0.727	0.434	0.484	0.504	0.575	0.549	0.715	0.745	0.739	0.734	0.703	0.720	0.752
Trace elements (ppm)															
Sn	nd	220	n.d.	164	259	252	192	231	220	n.d.	381	195	325	396	390
Rb	4.4	25	30	<3	<3	2.4	1.3	n.d.	n.d.	1.6	4.0	<2	n.d.	5.9	<2
Cs	1.0	4.1	8.7	1.7	0.48	1.4	1.0	n.d.	n.d.	0.40	1.0	0.78	n.d.	3.4	0.30
Sb	0.93	2.8	0.66	2.1	5.2	1.6	1.1	n.d.	n.d.	1.5	1.3	1.5	n.d.	1.0	2.2
Co	0.58	1.3	2.0	0.17	0.15	0.11	0.22	n.d.	n.d.	0.24	0.12	0.13	n.d.	0.20	0.15
Sc	2.2	2.2	0.30	0.060	0.065	0.035	0.035	n.d.	n.d.	0.025	0.020	0.020	n.d.	<0.04	0.060
La	5.1	11.0	1.7	0.93	0.46	0.23	0.080	n.d.	n.d.	0.045	0.040	0.14	n.d.	0.17	<0.2
Nb	1.3	2.5	3.2	2.2	2.2	0.37	0.1	n.d.	n.d.	<0.1	0.17	<0.1	n.d.	<0.1	<0.1
Ta	5.9	63	150	0.51	0.42	0.60	0.52	n.d.	n.d.	1.2	1.7	1.6	n.d.	1.8	1.3
U	0.82	2.5	2.2	1.4	1.5	0.30	<1	n.d.	n.d.	0.10	0.17	0.75	n.d.	0.16	0.14
Th	3.1	6.2	1.3	0.25	0.18	0.080	0.070	n.d.	n.d.	0.075	0.10	0.075	n.d.	0.12	0.090
Ta/Nb	4.5	25.2	46.9	0.23	0.19	1.62	5.2	n.d.	n.d.	12	10	16	n.d.	18	13
U/Th	0.26	0.40	1.69	5.6	8.3	3.75	14	n.d.	n.d.	1.3	1.7	10	n.d.	1.3	1.6
Rb/Cs	4.4	6.1	3.4	1.8	6.3	1.7	1,3	n.d.	n.d.	4	4	2.6	n.d.	1.7	6.7

Notes:
* Fe reported as FeO
** Cation formulae normalized to 6 silicons
*** Boron assumed to be stoichiometric
**** MgO < 0.10 determined by atomic absorption spectrometry
nd = not detected by microprobe
n.d. = not determined

Table 3—*Continued*

Zone	Wall zone (5)					Wall zone (4)		1st intermediate zone (7)		3rd intermediate zone (8)			Core Type 9	Core Type 10
Sample	E2 (Core) ⟶⟶⟶ (Rim)	*****	F5 (Core) ⟶⟶⟶ (Rim)		F1	E1b	B15	G'6b	G4c	B11	B5b	B8	D'1	S1
SiO_2	34.73	36.33	37.53	38.91	35.90	36.66	36.50	36.88	36.47	36.67	36.46	36.45	37.14	37.95
TiO_2	0.18	nd	nd	nd	nd	nd	nd	nd	0.04	0.27	0.19	0.18	0.10	nd
Al_2O_3	33.87	36.95	35.16	39.29	36.07	36.19	36.42	35.45	36.35	35.95	35.70	36.25	38.03	39.52
FeO (1)	9.36	4.48	6.27	2.14	5.07	4.84	4.30	5.61	8.25	4.37	4.04	4.21	0.92	0.02
MgO	nd	nd	nd	nd	0.06	0.01	<0.01	0.05	0.06	0.27	0.41	0.37	<0.01	<0.01
MnO	0.15	0.33	0.34	0.49	0.51	0.74	0.84	0.75	0.37	0.49	0.52	0.79	1.64	1.08
ZnO	0.75	0.44	0.39	0.38	0.34	1.57	1.41	0.48	1.08	0.07	0.18	0.21	1.09	0.18
CaO	0.06	0.18	0.06	0.63	0.13	0.11	0.14	0.04	0.04	0.14	0.18	0.14	0.27	0.59
Na_2O	2.06	2.42	2.45	1.97	2.60	2.33	2.26	2.85	2.35	2.40	2.63	2.43	2.05	1.70
K_2O	0.03	0.02	nd	nd	0.02	0.04	0.06	nd	nd	0.03	0.04	0.04	0.14	0.03
Li_2O	(0.68)	(1.37)	(1.21)	(1.80)	1.46	1.55	1.58	1.41	1.09	1.53	1.56	1.44	1.67	1.83
F	1.42	1.42	1.39	1.39	1.27	1.42	1.42	1.42	1.33	1.44	1.49	1.46	1.29	0.98
Total	**83.29**	**83.94**	**84.80**	**87.00**	**83.43**	**85.46**	**84.94**	**84.94**	**87.43**	**83.63**	**83.40**	**83.97**	**84.34**	**83.88**
Cations per formula unit														
Si (2)	6.000	6.000	6.000	6.000	6.000	6.000	6.000	6.000	6.000	6.000	6.000	6.000	6.000	6.000
B (3)	3.000	3.000	3.000	3.000	3.000	3.000	3.000	3.000	3.000	3.000	3.000	3.000	3.000	3.000
Al (Z)	6.000	6.000	6.000	6.000	6.000	6.000	6.000	6.000	6.000	6.000	6.000	6.000	6.000	6.000
Al (Y)	0.896	1.192	0.625	1.141	1.105	0.981	1.056	0.797	1.048	0.933	0.924	1.033	1.241	1.364
Ti	0.023	--	--	--	--	--	--	--	0.005	0.033	0.024	0.022	0.012	--
Fe	1.352	0.619	0.838	0.276	0.709	0.663	0.592	0.763	1.135	0.598	0.556	0.580	0.124	0.003
Mg	--	--	--	--	0.016	0.002	0.001	0.012	0.014	0.066	0.101	0.091	0.002	0.001
Mn	0.022	0.046	0.046	0.064	0.072	0.102	0.117	0.103	0.052	0.068	0.072	0.110	0.224	0.145
Zn	0.096	0.054	0.046	0.043	0.042	0.190	0.171	0.058	0.131	0.008	0.022	0.026	0.130	0.021
Li	0.473	0.910	0.779	1.115	0.981	1.020	1.045	0.923	0.722	1.007	1.032	0.953	1.085	1.164
Σ Y site	**2.862**	**2.821**	**2.334**	**2.639**	**2.925**	**2.958**	**2.982**	**2.656**	**3.107**	**2.713**	**2.731**	**2.815**	**2.818**	**2.698**
Ca	0.011	0.032	0.010	0.104	0.023	0.020	0.025	0.007	0.007	0.025	0.032	0.025	0.047	0.100
Na	0.690	0.775	0.759	0.589	0.843	0.740	0.720	0.899	0.750	0.761	0.839	0.776	0.642	0.521
K	0.007	0.004	--	--	0.004	0.008	0.013	--	--	0.006	0.008	0.008	0.029	0.006
Σ X site	**0.708**	**0.811**	**0.769**	**0.693**	**0.870**	**0.768**	**0.758**	**0.906**	**0.757**	**0.792**	**0.879**	**0.809**	**0.718**	**0.627**
F	0.776	0.742	0.703	0.678	0.671	0.735	0.738	0.731	0.692	0.745	0.775	0.760	0.659	0.499
Trace elements (ppm)														
	(average)		(average)											
Sn	349		552	379	344	425	400	260	359	442	293	526	600	
Rb	9.8		54	2.9	40	15	6.0	28	6.7	12	2.8	260	2.5	
Cs	0.50		8.4	0.60	4.9	2.1	1.4	6.6	2.1	4.4	18	33	0.40	
Sb	2.3		2.2	1.5	0.88	1.2	1.8	3.2	5.1	3.0	3.1	2.1	2.7	
Co	0.26		0.30	0.63	0.31	0.23	0.20	2.7	1.4	1.3	1.8	0.32	0.15	
Sc	0.045		0.065	0.065	0.020	0.010	0.080	0.14	0.28	0.23	0.22	0.013	<0.01	
La	<0.2		0.12	0.32	0.15	0.080	0.10	0.32	0.54	0.25	0.18	0.072	0.060	
Nb	0.12		<0.1	0.050	0.48	<0.1	0.04	<0.2	0.12	<0.1	0.13	0.51	0.060	
Ta	3.4		9.5	1.1	14	16	1.3	1.6	170	9.0	1.9	37	4.3	
U	<0.4		0.25	0.10	0.35	0.12	0.13	0.26	4.2	0.70	0.18	0.19	0.13	
Th	<0.1		0.17	0.13	0.16	<0.1	0.04	0.22	0.13	<0.1	0.040	0.12	0.23	
Ta/Nb	28		95	22	29	160	32.5	8	1417	90	15	73	72	
U/Th	4		1.5	0.77	2.2	1.2	3.25	1.18	32.3	7	4.5	1.6	0.6	
Rb/Cs	19.6		6.4	4.8	8.2	7.1	4.3	4.2	3.2	2.7	0.15	7.9	6.3	

Notes:
***** Samples E2 and F5 are strongly zoned on a fine scale, therefore extremes rather than averages are shown for for microprobe data.

Lithium values shown in () are calculated from linear regression based on Fe content.

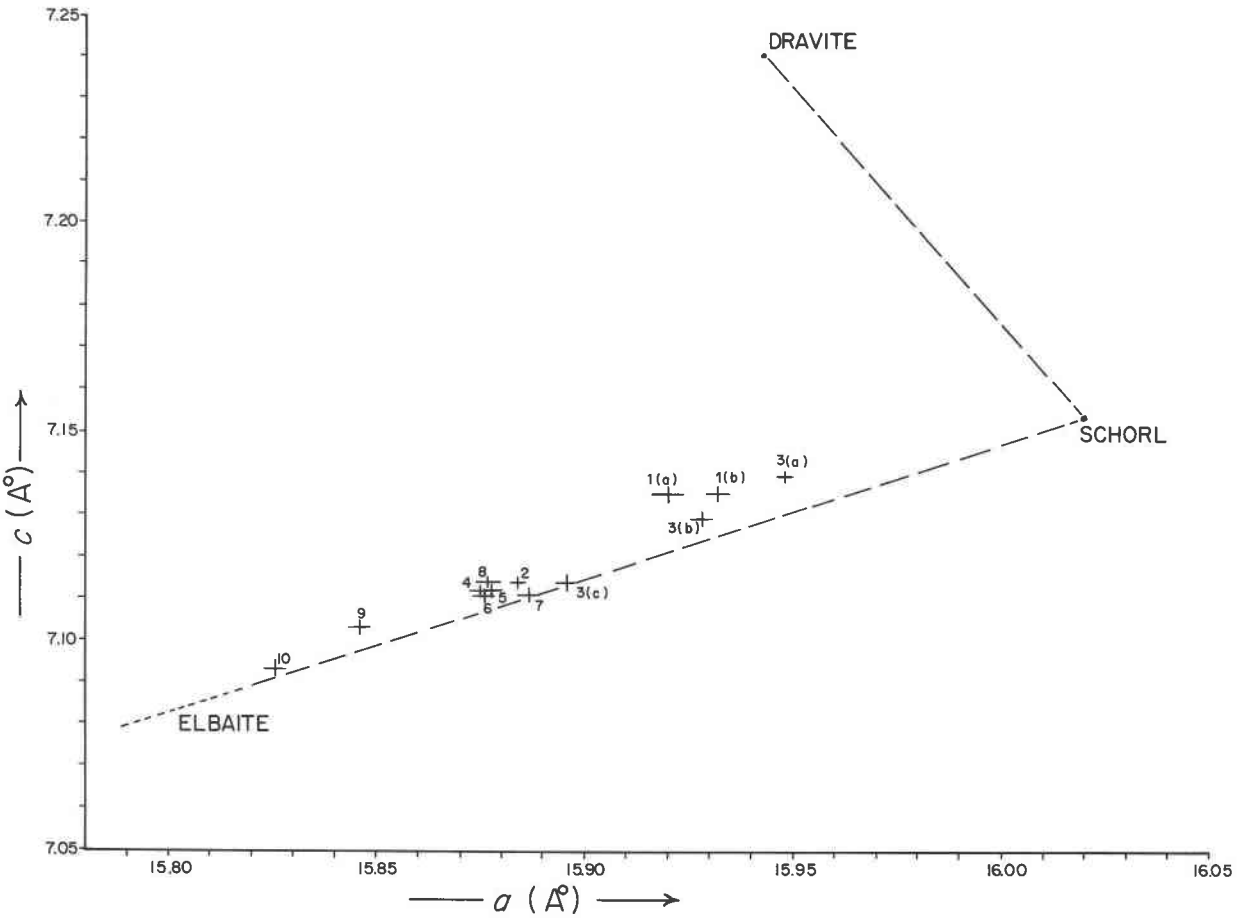

Fig. 6. Unit-cell dimensions of tourmaline samples representative of the ten textural types discussed in text. The size of each bar indicates $\pm 1\sigma$ error in the refined unit-cell dimensions. Dashed reference lines from Donnay and Barton (1972), modified from Epprecht (1953).

Tourmaline crystal chemistry and structure

Previous work on the tourmaline group of minerals is extensive. The structures of various tourmaline species have been solved and refined over the past three decades (Ito and Sadanaga, 1951; Buerger et al., 1962; Barton, 1969; Donnay and Barton, 1972; Fortier and Donnay, 1975; Foit and Rosenberg, 1979; Nuber and Schmetzer, 1979; Schmetzer et al., 1979; Nuber and Schmetzer, 1981; Schmetzer and Bank, 1984). Tourmaline compositions, although quite variable, may be represented by the general formula $XY_3Z_6(BO_3)_3Si_6O_{18}(OH,F)_4$. The tourmaline structure, illustrating site arrangement and coordination, is shown in Figure 10.

Table 4. Unit-cell dimensions of selected tourmaline samples from the Bob Ingersoll No. 1. dike

Type	Sample number	Color	a(A)	c(A)	V(A³)	Number of peaks used
1a	C'11	Brownish-black	15.924(4)	7.135(3)	1566.1(8)	23
1b	B7c	Brownish-black	15.932(3)	7.135(2)	1568.4(6)	26
2	B2	Brownish-green	15.884(2)	7.114(2)	1554.6(4)	25
3 (a)	E1a2	Bluish-black	15.948(2)	7.139(1)	1572.6(3)	22
3 (b)	B7a	Blue	15.928(3)	7.129(2)	1566.6(5)	30
3 (c)	D1	Blue	15.896(3)	7.114(2)	1556.7(6)	23
4	B15	Blue	15.875(3)	7.112(2)	1552.1(5)	30
5	F1	Blue	15.878(3)	7.112(2)	1552.8(5)	31
6	B7(1)	Green	15.876(3)	7.111(2)	1552.1(6)	27
7	G'6b	Blue	15.887(3)	7.111(2)	1554.4(6)	27
8	B8	Green	15.877(3)	7.114(2)	1553.1(5)	28
9	D'1	Bluish-gray	15.846(3)	7.103(2)	1544.5(5)	30
10	S1	Pink	15.826(3)	7.093(2)	1538.5(5)	28

One of the main compositional variables of tourmaline is the occupancy of the Y-site octahedra. In dravite, the Y-site cation is predominantly Mg; in schorl, Fe^{2+}; and in elbaite, Al and Li. The Y site may also contain substantial Fe^{3+} as in buergerite (Donnay et al., 1966), Mn (Schmetzer and Bank, 1984), V (Snetsinger, 1966; Foit and Rosenberg, 1979; Schmetzer et al., 1979), and Cr in chromian dravite (Dunn, 1977; Nuber and Schmetzer, 1979). The Z-site octahedra primarily contain Al but may cntain Fe^{3+} (Buerger et al., 1962; Frondel et al., 1966; Hermon et al., 1972; Walenta and Dunn, 1979), Cr^{3+} (Nuber and Schmetzer, 1979; Rumantseva, 1983), V^{3+} (Foit and Rosenberg, 1979), or Mg (Dunn, 1977; Schmetzer et al., 1979). In most varieties of tourmaline, Na is the dominant cation in the X site; however, appreciable Ca may be present as in uvite and liddicoatite (Dunn et al., 1977a,

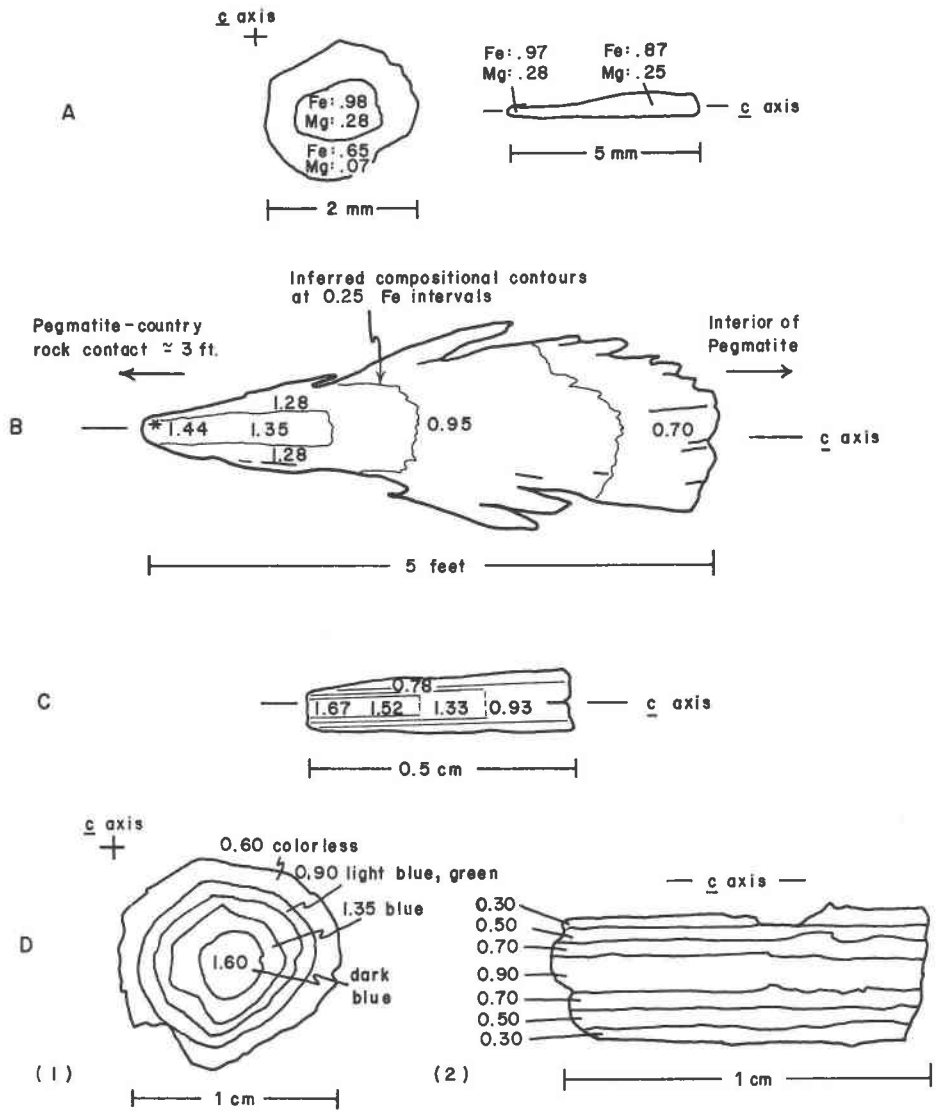

Fig. 7. Examples of compositionally zoned tourmaline crystals. Numerical values are Fe atoms per formula unit. Contours shown in B and C are schematic to illustrate inferred growth of crystals. Lines in D are boundaries between color-zones. (A) Tourmaline crystal of border zone (type 2) with high-Fe, high-Mg core. Longitudinal section shows variation of core composition along length (sample B2). (B) Longitudinal section of type 3 tourmaline crystal, showing spatial relation to pegmatite–country rock contact and growth direction toward interior of pegmatite (sample B7). (C) Type 3 tourmaline from exposure near top of dike (sample G11). (D) Type 5 tourmaline, with Fe-rich core and concentric zonation around the c axis. No variation occurs along the length of crystal shown in (2). [(1) Sample E2; (2) sample B16.]

1977b). Also, K and Mg may occur in minor amounts in the X site, or it may be partially vacant (Rosenberg and Foit, 1979; Werding and Schreyer, 1984). Tourmaline end-member compositions pertinent to this study appear in Table 5. B is generally assumed to fill the triangular-coordinated sites (e.g., Fortier and Donnay, 1975; Ekambaram et al., 1981; Schmetzer and Bank, 1984). Excess B may possibly substitute for Si (Barton, 1969); however, appreciable substitution of B for Si has not been documented.

Complete solid solution occurs between dravite and schorl, and nearly complete solid solution exists between schorl and elbaite (Foit and Rosenberg, 1977; Donnay and Barton, 1972). Compositions intermediate to the dravite and elbaite end members are not common although limited substitution does occur wherein Mg, Li, Al, and Fe occur together (Deer et al., 1962; El-Hinnawi and Hofmann, 1966; Chaudhry and Howie, 1976). There may be a miscibility gap between dravite and elbaite, or as suggested by Foit and Rosenberg (1979), the absence of intermediate compositions may be due to the fractionation of Li and Mg in natural geologic processes and fractionation by the tourmaline structure itself due to the sequence of cation field strengths.

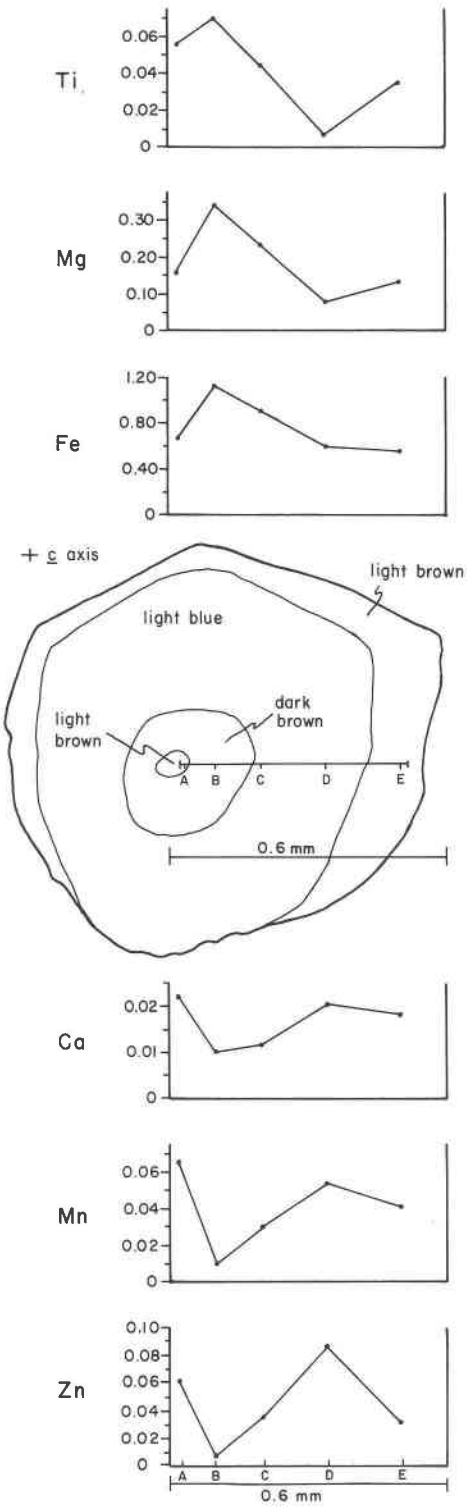

Fig. 8. Detailed compositional variation of zoned tourmaline crystal in border zone (type 2). Pleochroism as shown. Each point represents an average of two to four microprobe analyses in each zone.

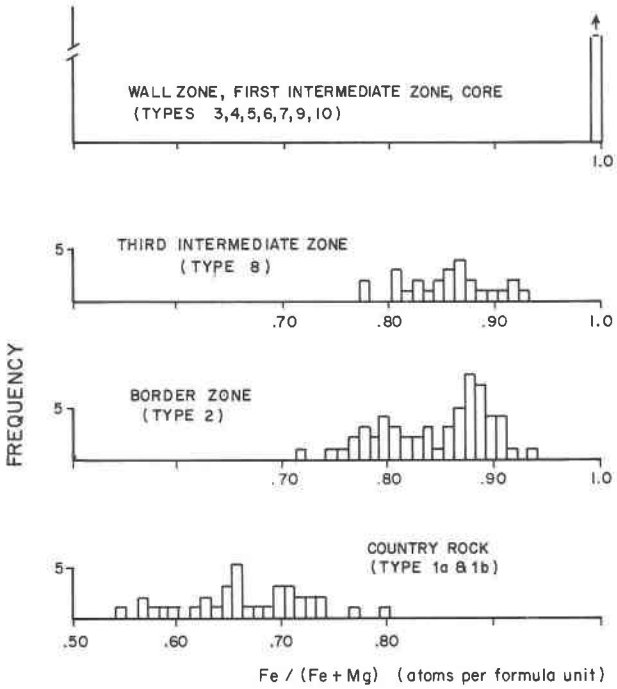

Fig. 9. Histograms showing range of Fe/(Fe + Mg) values for the different types of tourmaline.

Discussion

Tourmaline as a recorder

The first objective of this project was to determine whether the compositional variations of tourmaline at the Bob Ingersoll No. 1 pegmatite are systematic and are correlative with textures and mineral associations. As indicated by the values in Table 3, the compositional characteristics (major and minor element) of each textural type of tourmaline are different. Microprobe analyses of additional samples show similar compositional character for textural types represented by only one or two samples in Table 3 (see Figs. 15, 16). Smooth compositional variations within single tapered crystals, whose orientations indicate the direction of growth, clearly demonstrate the systematic nature of tourmaline compositional variation as the pegmatite-melt system crystallized (analogous to that of Foord, 1976). In addition, there is a general variation from the border zone to the core of the pegmatite involving Fe depletion and Li enrichment. Such variation is in accordance with the general fractionation behavior of these elements in magmatic systems and is in good agreement with previous studies of tourmaline in pegmatitic systems (Staatz et al., 1955; Foord, 1976).

The trace-element characteristics of the tourmaline are neither as consistent nor as systematic in variation as the major- and minor-element characteristics, with the exceptions of Sn, Co, and Sc. The Co and Sc vary similarly to Mg, whereas Sn generally increases with Li. There are several reasons for the nonsystematic concentrations of

the other trace elements. First, several of the elements are essential constituents of accessory minerals that occur in the pegmatite, such as Nb, Ta, and U in Nb-Ta oxides, including microlite. Others are strongly partitioned into mica and feldspar (Rb, Cs) and apatite (REE). For these trace elements, the abundance and distribution of the mineral in which they concentrate may complicate their distribution in tourmaline. The second problem results from the commonly poikilitic nature of the tourmaline. Even the purest crystals commonly contain microscopic solid inclusions, fracture fillings, and unidentified solids in abundant fluid inclusions (cf., Slivko, 1965).

The analysis of trace elements using bulk powders also precludes the determination of variations that probably occur in finely zoned crystals, based on the variations in major and minor elements. From the results shown in Table 3, it is apparent that compositional variations among the major and minor elements are the most useful for establishing trends. Certain trace elements may also be useful, but each element must be evaluated within the context of the mineralogy of the deposit.

Table 5. Selected tourmaline end-member composition

General formula	X	Y_3	Z_6	$(BO_3)_3$	Si_6O_{18}	$(OH,F)_4$
Dravite	Na	Mg_3	Al_6	$(BO_3)_3$	Si_6O_{18}	$(OH,F)_4$
Schorl	Na	Fe^{2+}_3	Al_6	$(BO_3)_3$	Si_6O_{18}	$(OH,F)_4$
Elbaite	Na	$(Li,Al)_3$	Al_6	$(BO_3)_3$	Si_6O_{18}	$(O,OH,F)_4$
Tsilaisite*	Na	$(Mn,Al)_3$	Al_6	$(BO_3)_3$	Si_6O_{18}	$(O,OH,F)_4$
Liddicoatite	Ca	$(Li,Al)_3$	Al_6	$(BO_3)_3$	Si_6O_{18}	$(O,OH,F)_4$
Uvite	Ca	Mg_3	Al_5Mg	$(BO_3)_3$	Si_6O_{18}	$(OH,F)_4$
Buergerite	Na	Fe^{3+}_3	Al_6	$(BO_3)_3$	Si_6O_{18}	$(OH)_3F$

Notes:
*Hypothetical end member

Compositional variation trends

As a first approximation of compositional trends, tourmaline samples may be listed in the following order: country rock–border zone–wall zone–first intermediate zone–third intermediate zone–core. The general trends of variation of the Y-site cations are shown in Figure 11. The major variation is a decrease in Fe^{2+} and an increase in Li + Al(Y), reflecting the dominant substitution $2Fe^{2+} \rightleftharpoons Li + Al$ in the Y site. Mg and Ti decrease sharply from the country rock to the border zone and then decrease to very low levels within the inner zones of the pegmatite. Zn and Mn show a general increase toward the core of the pegmatite, but with intermediate maxima and minima. Ca (X site) shows an increase toward the core, which is especially evident at low Fe concentrations (Fig. 17). The compositional trends of Y-site cations are shown in terms of major end-member compositions on a ternary dravite-schorl-elbaite composition diagram (Fig. 12).

The general compositional trends are related to the position of the tourmaline inward from the country-rock contact, as illustrated in Figure 13, which shows the same general trends as Figure 11, but also shows the trends of Mn, Zn, and Sn. Mn and Sn increase toward the core, while Zn initially increases toward the core but reaches a maximum in the inner wall zone near the core, then decreases. An increase in Sn concentration has been interpreted as an indicator of increasing fractionation of the melt (Power, 1968). The trends shown in Figure 13 clearly reflect an inward fractionation trend, and although the intermediate zones are not represented in this traverse (Fig. 13), the fractionation trends that may be expected from the wall to the core are here established. Furthermore, tourmaline samples from the border and wall zones from widely separated locations in the pegmatite are compositionally similar, which may suggest that initial differentiation of the pegmatite was caused by crystallization at the walls. Tourmaline samples from the intermediate zones, however, have compositional differences that may reflect vertical differentiation of the pegmatite.

The general compositional trends are in good agreement with the results of previous studies (e.g., Staatz et al., 1955; Foord, 1976; Manning, 1982). In accordance with these results, the major trend of decreasing schorl and dravite components, and of corresponding increase of elbaite component, appears to be a useful indicator of the relative degree of fractionation and the paragenetic sequence of the tourmaline and associated primary minerals.

A close inspection of Figure 11 reveals considerable overlap in values from the border zone, wall zone, and intermediate zones. The data points are averages of multiple microprobe analyses, and Li values are obtained from bulk crystal powders. These trends may be studied in more detail by considering individual microprobe analyses. Although Li cannot be determined by microprobe analyses, the good inverse correlation of Li and Fe [or (Fe + Mg)] provides a basis for the use of (Fe + Mg) as an index of relative evolution or paragenesis. Each individual microprobe analysis can be plotted against this index to show the covariation of the cations and thus demonstrate any systematic variations with progressive evolution of the tourmaline. Also, by using (Fe + Mg) rather than Li, the compositional variations in fine-grained, zoned crystals may be compared with trends among tourmalines of the different types. In summary, the ideal evolutionary trend would be reflected by values of (Fe + Mg) or [Li + Al(Y)] normalized to Σ[Fe,Mg,Li,Al(Y)]; however, because Li cannot be determined directly, the value of (Fe + Mg) may be used as the best approximation.

The (Fe + Mg) range of each of the types of tourmaline may be used to illustrate their paragenetic sequence (Fig. 14). Although this diagram indicates extensive overlap of the various tourmaline types and broad ranges of (Fe + Mg) content, there are systematic compositional zonation trends that account for much of the apparent range or scatter of the data. For example, in the wall zone, high-

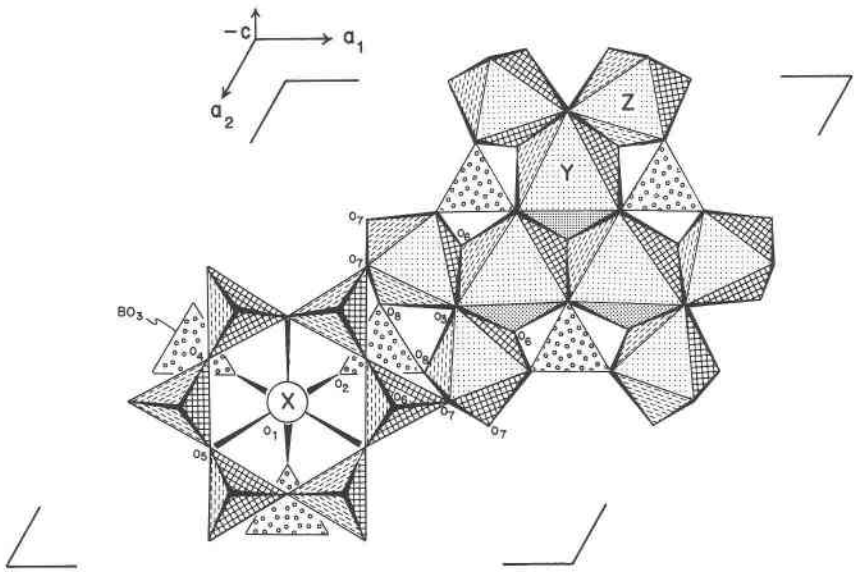

Fig. 10. Portion of the structure of tourmaline projected onto (0001), looking up the c axis. Drawn from atomic coordinates of the refined de Kalb tourmaline, given by Buerger et al. (1962); $a = 15.95$ Å, $c = 7.24$ Å. Symmetry-related anion positions shown as O_1–O_8. Additional BO_3 groups shown for clarity.

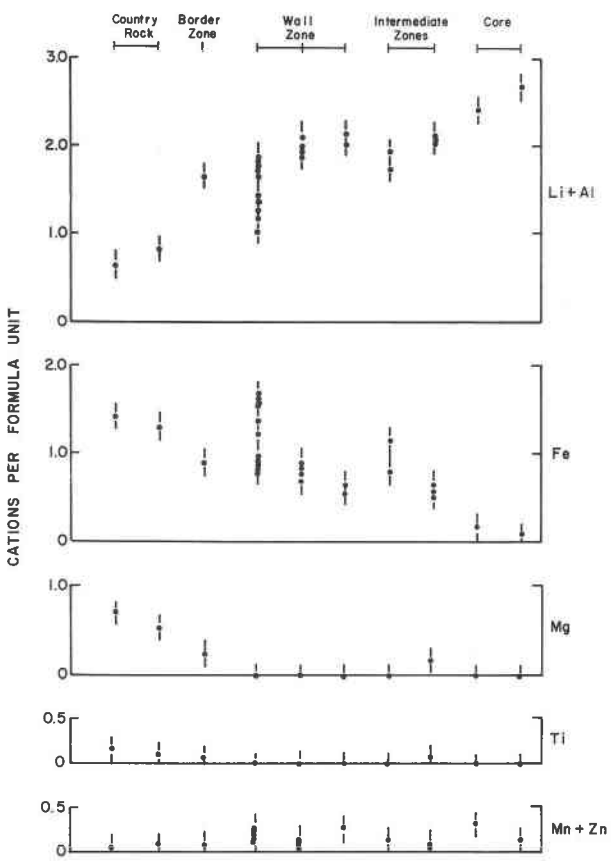

Fig. 11. General compositional variations of the Y-site cations in tourmaline of the Bob Ingersoll No. 1 dike. Data points represent averages of multiple microprobe analyses.

Fe tourmaline occurs toward the outer portions of the zone grading to low-Fe tourmaline toward the interior portions (Fig. 16a). In addition, many individual crystals are strongly zoned, as noted previously, contributing to the range of compositions observed for each textural type.

Zoning of individual crystals

The compositional variations in individual zoned crystals are of particular interest as they mirror variation trends within suites of texturally similar tourmalines. One common cause of compositional zoning is rapid crystal growth (Zoltai and Stout, 1984) during which the diffusion rates of select components do not keep pace with the rate of crystallization. This may have been the case for the border zone crystals (e.g., Fig. 8). The compositional zoning is not simply a smooth variation, but involves a repetitious sequence that may result from one or several changes in the rate of crystallization. The initial Mg-, Fe-, and Ti-depleted core of the crystal shown in Figure 8 may have resulted from an initial abrupt increase in the liquidus temperature of the pegmatite melt. If sufficiently abrupt, a substantial difference between the liquidus and melt temperatures might cause the crystallization of an unstable tourmaline solid solution at a composition intermediate to the stable coexisting liquid and solid compositions, as suggested by Dowty (1980) and Lofgren (1980). Following the nucleation of the unstable composition, additional crystallizing layers obtain the equilibrium composition. This zoning phenomenon may be repeated if another temperature change occurs, such as from the rapid loss of volatiles from the melt (Lofgren, 1980). The rapid or sporadic loss of volatiles, such as by a pulse of exsolving fluid from an H_2O-saturated melt of the border zone would also provide an efficient removal of latent heat of crys-

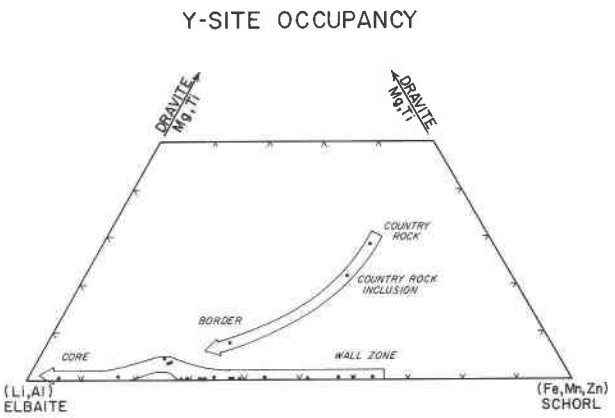

Fig. 12. End-member compositions of the Bob Ingersoll tourmaline plotted in terms of schorl (Fe + Mn + Zn), dravite (Mg + Ti), and elbaite (Li + Al).

tallization and possibly a local pressure drop, causing rapid disequilibrium crystallization.

Alternatively, border-zone crystallization may have begun when the pegmatite melt reached a pressure–temperature regime favorable for aqueous-fluid exsolution. With the first pulse of fluid, the liquidus would have been raised, initiating border-zone crystallization. Compositional variations in the border-zone tourmaline may reflect different element partitioning in a mineral-melt system versus a mineral-melt-fluid system; therefore, if fluid exsolution during border-zone crystallization occurred in pulses, then the tourmaline would contain repetitious zoning.

Another common cause of zoning is the change of intensive variables—pressure, temperature, or composition of the crystallizing medium—during the normal course of crystallization (i.e., not necessarily as a result of rapid crystallization). Changes in lithostatic pressure were probably not important because the pegmatite was emplaced at 3 kbar or greater (Redden et al., 1982); however, variations in P_{H_2O} may have been an important factor. The smooth compositional variation within single crystals of type 3 tourmaline in the wall zone (Figs. 7, 16a) reflect either changes in the composition of the closed melt-fluid system with progressive crystallization or a slowly decreasing temperature, or both. The zoning observed in type 5 crystals appears to have resulted from the depletion of Fe in particular, as progressively more evolved fluids permeated the wall zone.

The changing composition of the pegmatite melt-fluid system with progressive crystallization is closely related to (and in part caused by) the stability of a given tourmaline composition at a particular set of pressure-temperature conditions. For example, at high temperatures, Fe-rich compositions are more stable than Li-rich compositions; thus, early tourmaline crystallization contributes to the Fe-depletion of the melt. Although tourmaline solid solution is complex, tourmaline may be expected to behave similarly to other minerals with octahedral sites.

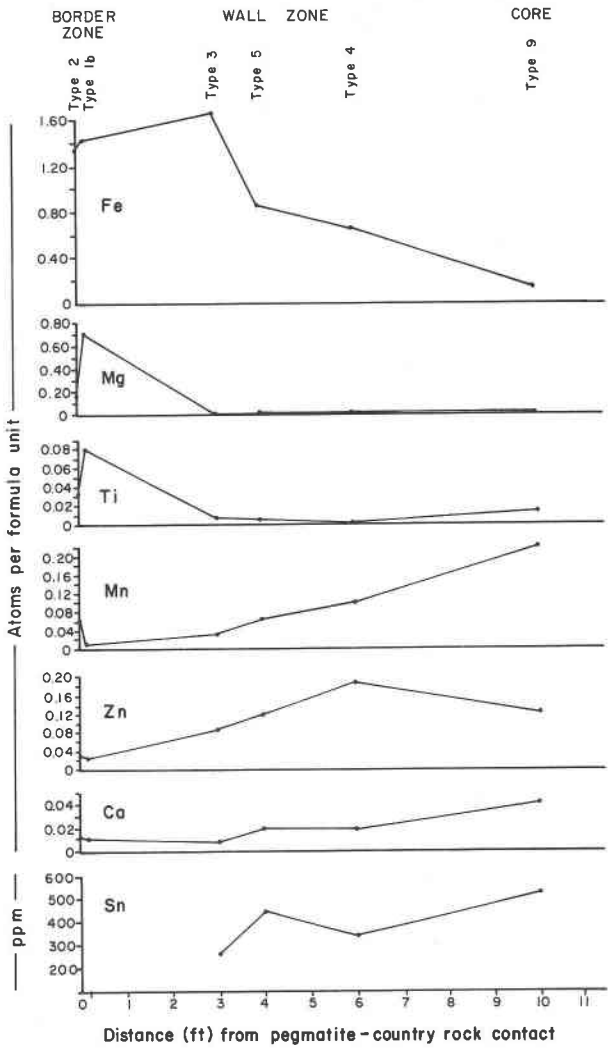

Fig. 13. Compositional variation with respect to distance from country-rock contact. Representative samples from west-central part of Bob Ingersoll No. 1 dike as follows: type 1b, country-rock inclusion, G11(a); type 2, border zone, G11(b); type 3, wall zone, coarse, E1a2; type 5, wall zone, intergrown with muscovite, E1a1; type 4, wall zone, fine, E1b; type 9, core, D'1. (First and second intermediate zones absent in this area; third intermediate zone is thin and contains no tourmaline.)

Of the major Y-site cations, Mg should be preferred at higher temperatures, Fe at intermediate, and Li at lower temperatures based on ionic size and charge (Tauson, 1965). It is therefore important to consider (and to identify) the different effects of simple depletion or enrichment of elements in the melt-fluid versus crystal-chemical stability under varying conditions.

Crystal-chemical control of tourmaline composition

The initial purpose of Figures 15 through 17 was to illustrate how Mg and the four transition metals Ti, Fe, Mn, and Zn covary as the pegmatite crystallized, under the premise that decreasing (Fe + Mg) is a good index of

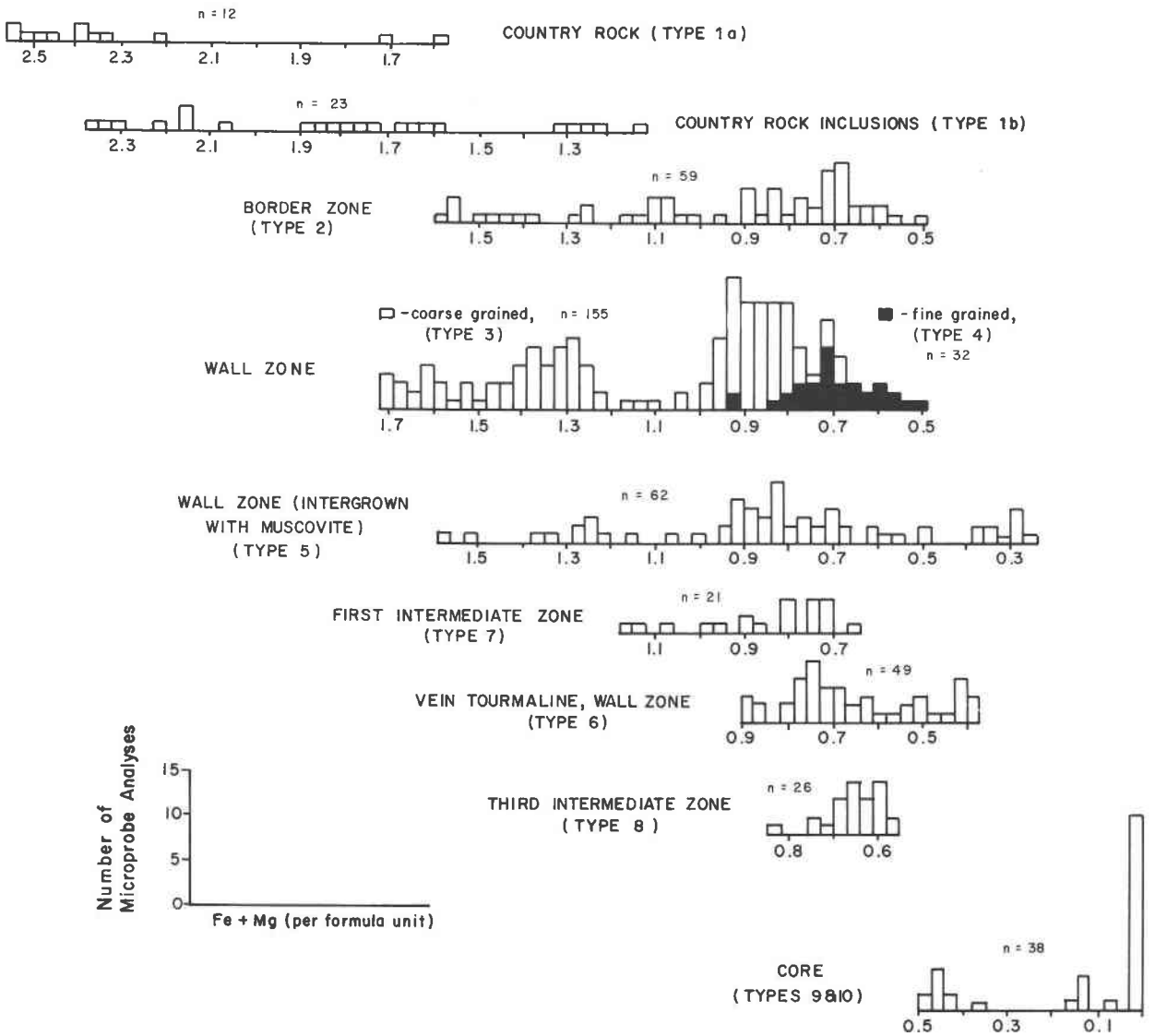

Fig. 14. Tourmaline paragenesis based on (Fe + Mg) values (atoms per formula unit), shown along abscissa; n = the number of analyses for each group.

progressive crystallization. Owing to the similarity of their properties, these cations should generally behave as ferromagnesian elements, and thus each should in turn decrease as Li increases. The sequence in which these five elements should first peak, then diminish as temperature falls during crystallization can be predicted, as suggested by Foit and Rosenberg (1979). Under ideal melt conditions (no effects from cocrystallizing phases, no other fractionation processes), the cation with the highest field strength should be favored at high temperature and the cation with the lowest field strength, at low temperature. Thus in an ideal crystallization sequence, the elements might covary as shown schematically in Figure 18. Cations with successively lower field strengths should ideally be at their peak concentration in tourmaline at successively lower temperatures, if their concentrations in the melt are of a similar order of magnitude (Tauson, 1965; Foit and Rosenberg, 1979).

The cation field strength may be approximated by Z/r^2 in which Z = charge and r = cation radius for octahedral coordination. Using Zhdanov's (1965) values for the ionic radii in octahedral coordination (in Bloss, 1971), the approximate field strengths are Ti, 9.8; Mg, 3.7; Fe, 3.1; Zn, 2.9; and Mn, 2.4. Figure 18 is drawn such that the quantity of each element is similar to the quantity actually observed in tourmaline from the pegmatite, that is, Fe and [Li + Al(Y)] are the principal substituents, and Mg, Ti, Zn, and Mn are subordinate. The (Li + Al) couple may be explained by the same reasoning if the field strength of Li (~2.1) is the governing factor. Al has a high field strength

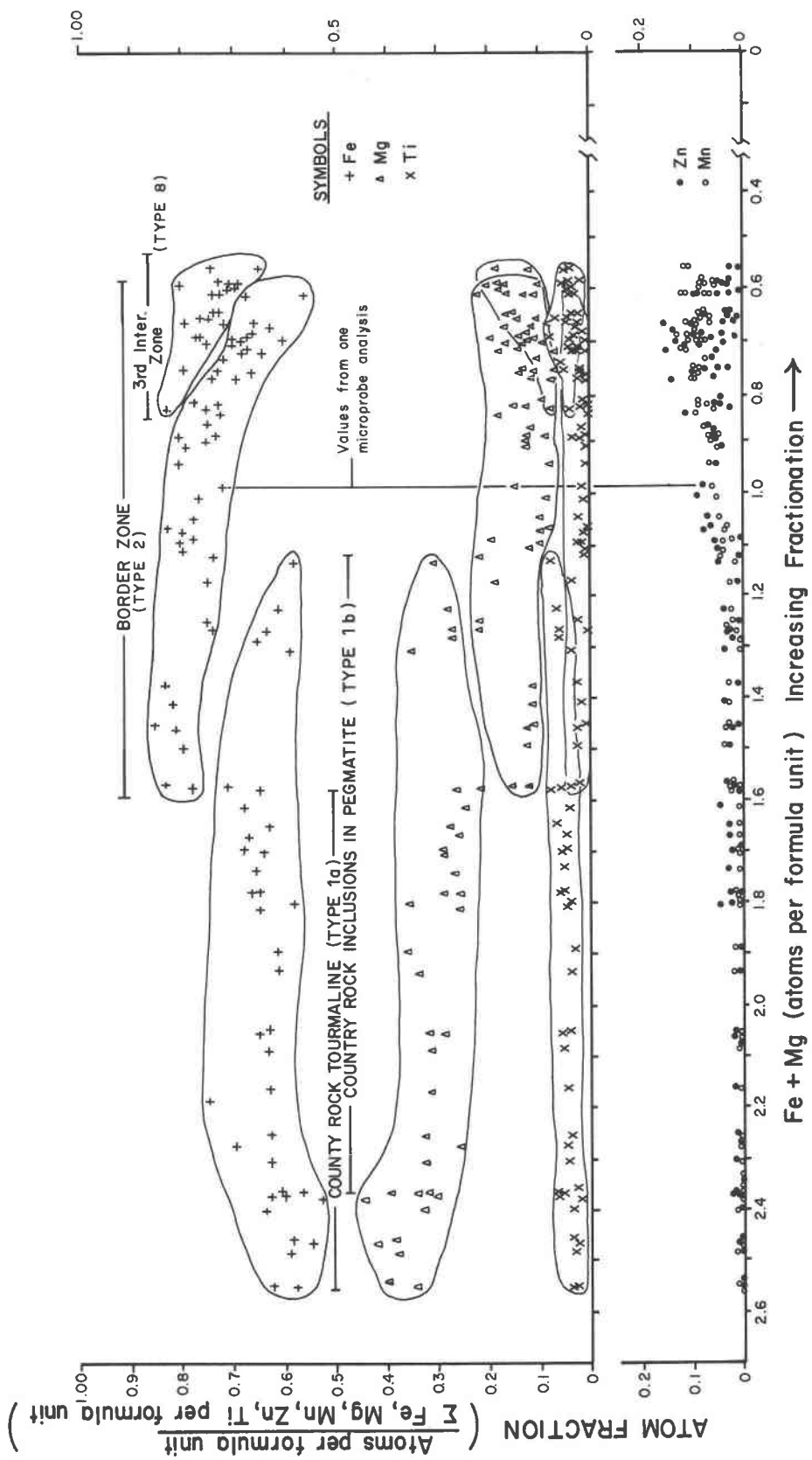

Fig. 15. Compositional trends of types 1, 2, and 8 tourmaline in terms of atom fractions of Fe, Mg, Ti, Mn, and Zn versus (Fe + Mg) (atoms per formula unit). Each symbol represents the appropriate atom fraction for a single microprobe analysis.

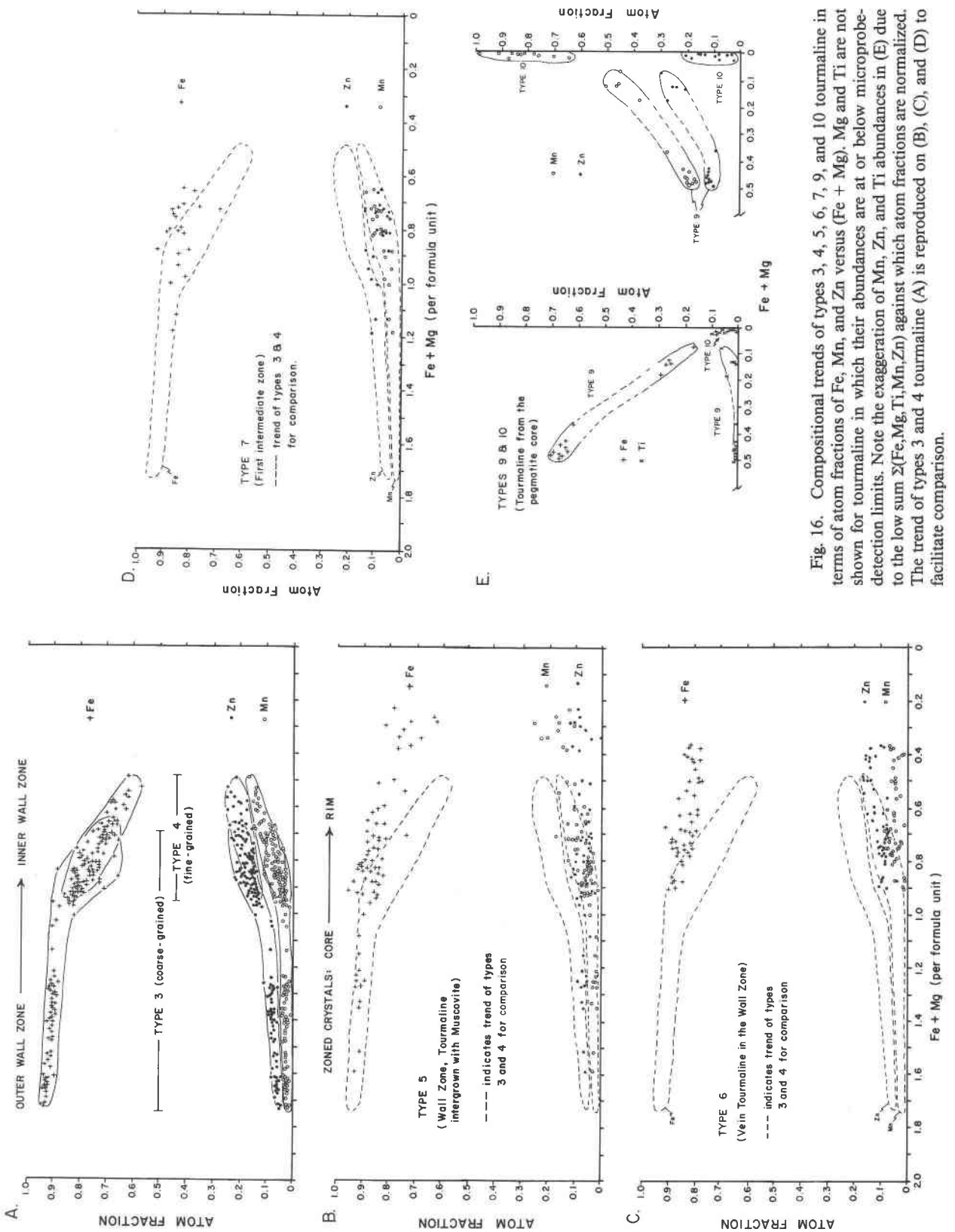

Fig. 16. Compositional trends of types 3, 4, 5, 6, 7, 9, and 10 tourmaline in terms of atom fractions of Fe, Mn, and Zn versus (Fe + Mg). Mg and Ti are not shown for tourmaline in which their abundances are at or below microprobe-detection limits. Note the exaggeration of Mn, Zn, and Ti abundances in (E) due to the low sum Σ(Fe,Mg,Ti,Mn,Zn) against which atom fractions are normalized. The trend of types 3 and 4 tourmaline (A) is reproduced on (B), (C), and (D) to facilitate comparison.

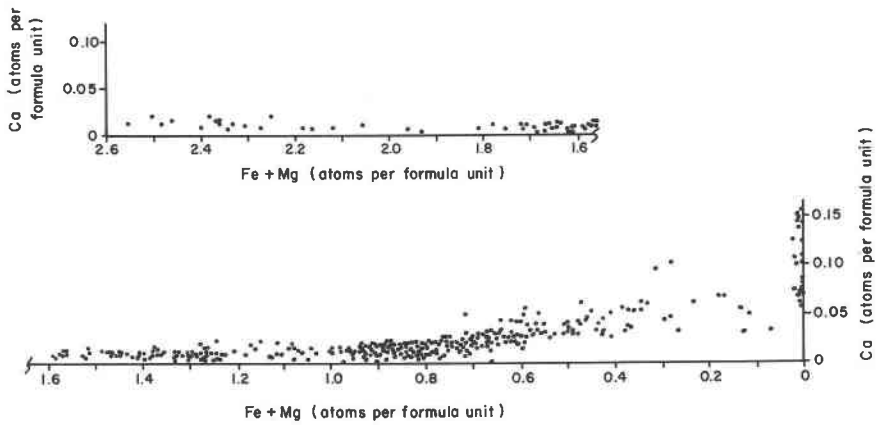

Fig. 17. Variation in concentration of Ca in Bob Ingersoll tourmaline in terms of Ca atoms per formula unit vs. (Fe + Mg).

and thus readily fits the Y-site octahedra, its concentration apparently limited only by charge-balance requirements.

Figure 19 is similar to Figure 18, but is constructed from compositional data in Table 3. The similarity of trends shown in Figures 18 and 19 indicates the importance of crystal-chemical control of composition as an influencing factor on the overall compositional trends of the tourmaline. Recognition of this factor allows further interpretations regarding additional factors, such as differentiation due to the coexistence of melt and aqueous fluid, or the fractionation effects of other crystallizing minerals.

Processes of crystallization

One of the foremost goals of this research is to determine whether aspects of tourmaline composition and texture or habit reflect the nature of the media from which the tourmaline crystallized. Three possibilities are suggested by three distinct trends of Fe and Mg variation, as follows: boron metasomatism, crystallization from silicate melt, and crystallization from a melt–aqueous fluid system.

The first trend of Fe-Mg variation is that of tourmaline in the country rock and in inclusions of country rock in the pegmatite. Such tourmalines exhibit a range of Fe/(Fe + Mg) from 0.544 to 0.799 (Fig. 9), with the lowest values generally corresponding to the highest (Fe + Mg) values. The lowest Fe/(Fe + Mg) values obtained for tourmaline appear to result from early replacement of biotite, prior to extensive re-equilibration with pegmatite fluids enriched in Fe relative to Mg. As the biotite re-equilibrated, its Fe/(Fe + Mg) value increased, as did that of tourmaline replacing biotite. Thus the zoned tourmaline in the country rock formed with low Fe/(Fe + Mg) cores that were mantled and thus protected from later re-equilibration by rims of successively higher Fe/(Fe + Mg). The biotite re-equilibrated completely, whereas the history of the re-equilibration was retained in the zoned tourmaline.

The second trend is characteristic of tourmaline from the pegmatite border zone. The Fe/(Fe + Mg) values range from 0.718 to 0.938, but there is actually very little overlap between these values and values for country-rock tourmaline (Fig. 9). Border-zone tourmaline crystals are zoned, with high-Fe, high-Mg cores, and the Fe/(Fe + Mg) ratio increases as (Fe + Mg) decreases (e.g., Fig. 7a). One inference is that this Fe/(Fe + Mg) ratio is governed by the Fe and Mg content of the pegmatite melt. Alternatively, the border-zone tourmaline may have been uniformly contaminated by Mg of the country rock, and the value of Fe/(Fe + Mg) a function of the equilibrium at the prevailing pressure, temperature, and composition. In any case, the Fe/(Fe + Mg) ratios reflect different processes of formation: country-rock tourmaline formed by boron metasomatism of Fe-Mg minerals in the country rock, and border-zone tourmaline by crystallization from a melt or fluid-melt system.

The third trend of tourmaline compositions on the basis of Fe and Mg values is that of samples of tourmaline interior to the border zone (with the exception of the third intermediate zone, discussed separately). All such tourmalines consistently contain Mg in quantities below 0.10

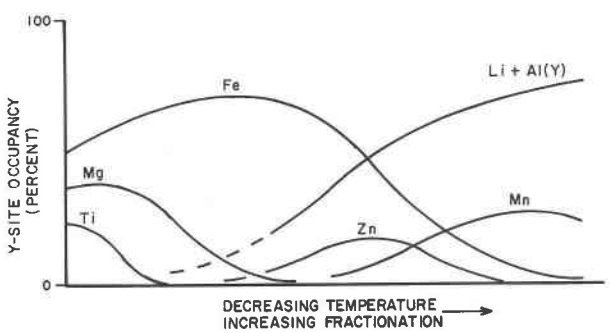

Fig. 18. Schematic illustration of ideal covariation of Y-site cations of tourmaline in response to decreasing temperature and increasing fractionation of melt.

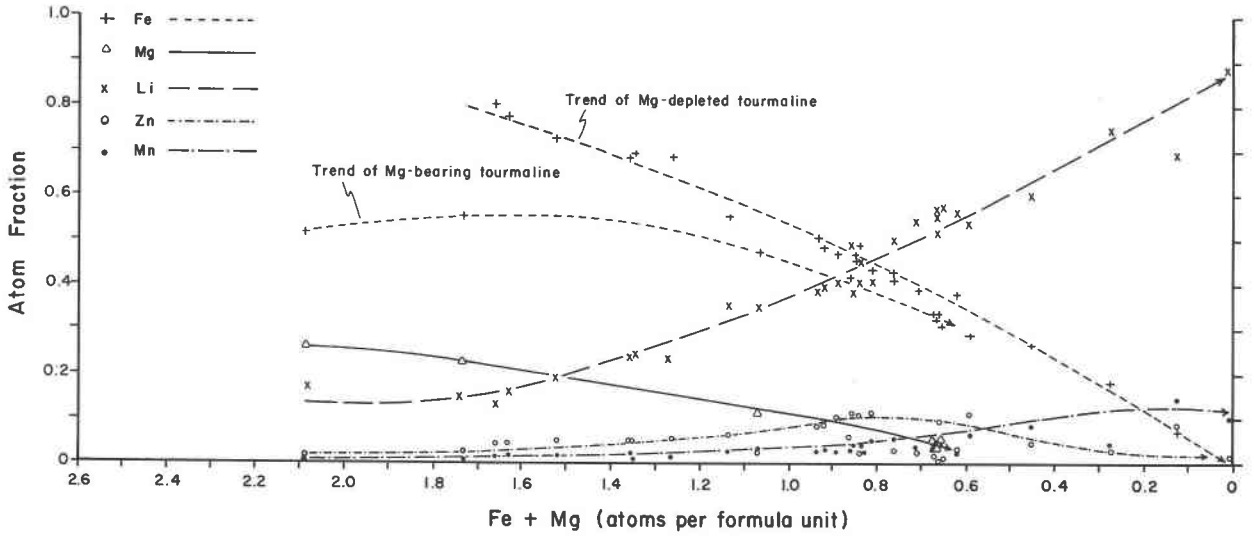

Fig. 19. Covariation of Y-site cations of Bob Ingersoll tourmaline with decreasing (Fe + Mg). Abscissa plotted as Fe + Mg as an approximation of increasing fractionation of the melt-fluid system. Data are from Table 3 (cf. Fig. 18).

wt% MgO (and most below 0.01). To further emphasize this, crystals that contain less than 0.10 wt% MgO occur in the wall zone within inches of the border zone (Table 3). Values of FeO in these same tourmaline samples, however, are greater than FeO values of border-zone tourmaline. It is proposed that the differentiation of Fe and Mg is due to the presence of an exsolving aqueous fluid. This is supported by the very coarse grain size of tourmaline immediately interior to the border zone (outer wall zone). The coarse grain size may be attributable to enhanced diffusion and crystal growth in an aqueous medium (Jahns, 1953, 1982).

Other compositional aspects of tourmaline in the third trend (Mg depleted) provide evidence of crystallization from a fluid-melt system that was differentiated relative to the border zone. Aside from Mg depletion, Zn and Mn become enriched as Fe decreases with inward crystallization of the wall zone (Fig. 16a). Additionally, Fe, Mn, and Zn concentrations constitute well-defined trends as Fe decreases, implying that these elements were efficiently differentiated and approached the ideal crystal-chemical concentration in tourmaline at the given pressure, temperature, and composition of the crystallizing medium. These trends and the habit of tourmaline in the outer wall zone may indicate the presence of an aqueous-fluid interface between melt and crystallizing tourmaline. Alternatively, exsolved fluid rising through the melt may have caused differentiation by depleting lower portions of melt of the elements that favor the fluid, thus enriching melt in upper parts of the pegmatite in these same elements. Evidence supporting this process is the occurrence of type 3 tourmaline predominantly on the hanging wall of the pegmatite.

The differentiation of an aqueous fluid exsolving from the silicate melt should have several effects on tourmaline compositions. Certain elements such as Zn and Mn should favorably partition into the aqueous fluid from the silicate melt and thus be enriched in the tourmaline. Holland (1972) found Zn and Mn to be enriched in the aqueous fluid (Zn > Mn) in the presence of Cl. Fe is also favorably partitioned into aqueous fluid coexisting with silicate melt (Burnham, 1979), but Mg is strongly retained in the melt (Holland, 1972). Another effect on composition of crystallizing tourmaline results from the increased diffusivity of elements in an aqueous phase, the viscosity of which may be seven orders of magnitude less than the silicate melt (Jahns, 1982). With increased diffusivity, diffusing ions should respond more efficiently to chemical potential gradients, and therefore the composition may approach the ideal crystal-chemical-controlled (equilibrium) concentrations of each of the elements involved in tourmaline substitution.

The halogens F and Cl should also show characteristic partitioning behavior in the presence of aqueous fluid and silicate melt. Cl concentrates in the fluid, and F preferentially remains in the melt (Hards, 1976; Fuge, 1977; Burnham, 1979; Manning, 1981). The ratio of these elements in tourmaline should therefore provide insight as to the presence of aqueous fluids; however, Cl has not been determined in this study. F contents (Table 3), which are lowest in tourmaline of the outer wall zone, indicate that the crystallization of this tourmaline (type 3) may have occurred in the presence of an aqueous-fluid interface between the growing tourmaline and silicate melt, or that the crystallizing medium was diluted with respect to F by an abundance of aqueous fluid.

On the basis of the F content of all the tourmaline of the Bob Ingersoll No. 1 dike, the pegmatite is F-rich (cf.,

Nemec, 1969). Amblygonite-montebrasite in the Bob Ingersoll No. 1. dike contains ~3 wt% F ($X_{Amb} \cong 0.25$), and lepidolites contain as much as 7 wt% F (F/OH $\geq$ 0.8). From the preponderance of fluorapatite over chlorapatite in Black Hills pegmatites in general (Roberts and Rapp, 1965; Papike et al., 1984), the pegmatite was probably not enriched in Cl (e.g., F $\cong$ 3–4 wt%, Cl < 0.01 wt% in apatite, Jensen, 1984; cf., Roegge et al., 1974). It follows that although elements such as Zn and Mn were enriched in the aqueous fluid, the enrichment was only by a small factor and they were not completely extracted from the melt.

There is also textural evidence from the coarse tourmaline of the outer wall zone (type 3) for the presence of an aqueous fluid during crystal growth. External, heterogeneous nucleation of these crystals, with the inward-crystallizing wall of the magma chamber as the substrate, is indicated by both the paucity and irregular distribution of crystals, and also by their orientation relative to the wall (Lofgren, 1980). Such nucleation characteristics combined with the very coarse grain size suggests crystallization in the presence of a medium of reduced viscosity, e.g., melt and exsolving aqueous fluid. Additionally, the orientation of type 3 tourmaline crystals is analogous to an extremely coarse grained variant of comb layering, the origin of which has been similarly interpreted (Moore and Lockwood, 1973).

The trend of Mn and Zn enrichment in tourmaline concomitantly with progressive crystallization of the wall zone (Fe depletion), holds well for coarse-grained (type 3) and fine-grained (type 4) tourmaline of the wall zone. Although texturally different, the similarity of trends indicates a similar crystallization mechanism for both. The fine-grained tourmalines simply grew at a stage when much of the surrounding portion of the wall zone had previously crystallized, consistent with their occurrence in the interior parts of the wall zone and their subhedral texture. The location of the fine-grained crystals and the orientation of coarse-grained crystals perpendicular to the border zone–wall zone contact are evidence of an orderly inward crystallization of the wall zone. However, tourmaline that occurs with coarse-grained segregations of muscovite in the wall zone (type 5) deviates somewhat from the trend (Fig. 16b). Some of these crystals are strongly zoned (Fig. 7d), commonly with rims very low in Fe. At high Fe values, Zn and Mn fall on the main wall-zone trend (see Fig. 16b), whereas at values between 1.0 and 0.7 Fe atoms per formula unit, Zn and Mn are generally low relative to other wall-zone tourmaline. This may be due in part to the phengitic nature of the coexisting muscovite (Table 6). Although muscovite may incorporate substantial amounts of the Y-site cations of tourmaline, the amounts are quite variable. Cation exchange with muscovite as the tourmaline crystallized may have buffered the Mn and Zn concentrations, as fluids became progressively more Fe depleted. It is evident from the range of Fe contents of different samples of type 5 tourmaline that the crystallization of this assemblage occurred throughout the crystallization of the wall zone (Fig. 14).

Table 6. Values of selected oxides for coexisting tourmaline and muscovite

Sample number	*FeO		MgO		MnO		ZnO		Zone	Tourmaline type
	T**	M***	T	M	T	M	T	M		
G1	4.67	0.97	0.48	0.33	0.52	0.15	0.43	0.17	Border	2
Bbb	6.79	<0.01	0.01	<0.01	0.29	0.12	1.27	0.42	Wall	3
G11	6.02	0.72	<0.01	<0.01	0.69	0.17	1.37	0.26	Wall	3
C7b	5.96	0.24	<0.01	<0.01	0.21	0.03	0.78	0.05	Wall	5
E1a1	5.88	0.91	0.02	0.02	0.44	0.08	0.94	0.06	Wall	5
B1b	5.10	0.95	<0.01	0.05	0.59	0.04	0.39	0.05	Wall	5
F5	2.95	0.78	0.01	0.01	0.52	0.07	0.37	0.14	Wall	5
C1	5.62	0.80	<0.01	<0.01	0.39	0.05	1.22	0.11	Wall	4
E1b	4.84	0.64	0.01	0.01	0.74	0.05	1.57	0.09	Wall	4
G4c	8.25	0.63	0.06	0.03	0.37	0.04	1.08	0.06	1st Int.	7
B12	3.50	0.13	0.47	<0.01	0.38	<0.01	0.13	0.03	3rd Int.	8
D'1	0.92	0.07	<0.01	<0.01	1.64	0.23	1.09	0.06	Core****	9

Notes:
* Values are in wt.%
** T - tourmaline
*** M - muscovite
**** D'1 mica is lepidolite: $Li_2O \cong 4$ wt.%, F $\cong$ 5 wt.%

Tourmaline of the first intermediate zone (type 7) is compositionally similar to type 5 tourmaline (Fig. 16d). The range of Fe concentrations suggests an overlapping paragenesis with wall-zone tourmaline; however, the compositional trends of tourmaline from this zone may be incomplete owing to sampling restrictions imposed by previous mining of the interior parts of the zone. Tourmaline was not an early-forming mineral in this zone, based on its occurrence as an anhedral constituent of the matrix between feldspar megacrysts. This suggests crystallization from the interstitial, residual melt following early K-feldspar crystallization. The residual nature of the liquid is supported by a slight Mg content, and by elevated Sc and Co concentrations of one of the samples (G4c, Table 3).

Tourmaline from the third intermediate zone (type 8) is compositionally similar to border-zone tourmaline (Fig. 15) and almost identical to the outer rim of the crystal in Figure 8 except that Mn and Zn are depleted relative to the border-zone tourmaline. Type 8 tourmaline is enriched in Mg, Co, Sc, and F and depleted in Fe, Mn, and Zn relative to type 3 tourmaline. On the basis of the fractionation of these elements between coexisting silicate melt and aqueous fluid, as discussed earlier, it appears that this composition reflects crystallization from a residual magma that had previously undergone aqueous-fluid separation. Additionally, the distribution of the tourmaline crystals is regular, and they have no preferred orientation (Fig. 5b), both of which support homogeneous nucleation and growth directly from the melt (Lofgren, 1980). This raises the question of how exsolution of aqueous fluid can cease once it has begun in a saturated melt.

A saturated granitic melt should contain at least ~10 wt% H_2O at 3 kbar (Tuttle and Bowen, 1958); therefore once saturated, the crystallization of any minerals, all of which contain less than 10 wt% H_2O, should cause the

remaining melt to be continuously oversaturated. However, from recent work by London (1986), the solubility of H_2O in a silicate melt may be increased significantly by the buildup of an alkali borate (specifically $Li_2B_4O_7$) component in the melt. This may have been the case in the third intermediate zone in which tourmaline occurs only at the inner contact with the core. Otherwise, the third intermediate zone consists of a barren assemblage of quartz and Na-feldspar. The reason for tourmaline instability throughout most of the zone is unclear, although the coordination state of B^{3+} in the melt may be a factor (Chorlton and Martin, 1978; Pichavant, 1981; London, 1986). The implication is that in the absence of tourmaline crystallization, the activities of Li, F, and B in the melt increase and thus allow increased solubility of water. This results in melt depolymerization (Burnham, 1979) and thus an increase in the availability of structural sites in the melt for network-modifying cations. When tourmaline becomes stable and crystallizes, the $Li_2B_4O_7$ component is removed from the melt, water exsolves, and a diverse mineral assemblage results from the loss of structural sites in the melt (London, 1986). The presence of the accessory-mineral assemblage of tourmaline, beryl, apatite, and cassiterite at the contact of the third intermediate zone and the core supports this model.

The Mg content of type 8 tourmaline poses a problem relating to the enrichment of Mg during the crystallization of the pegmatite. The normal compositional variation with progressive crystallization in a magmatic system should include Mg depletion. If the Mg content of the melt is progressively depleted following border-zone crystallization, how then does type 8 tourmaline form with the same Fe/(Fe + Mg) as border-zone tourmaline? This may result from an increase in Mg concentration in residual melt during the hiatus in tourmaline crystallization at the time of formation of the third intermediate zone and from the preferential loss of components other than Mg to previously exsolved aqueous fluid.

The similarity of Fe/(Fe + Mg) values between types 2 and 8 tourmaline raises another question: is Fe/(Fe + Mg) in tourmaline temperature dependent in a given system, e.g., melt-crystals? If so, the temperature of crystallization of the border zone may have been nearly the same as that of the third intermediate zone. This may be possible if the border zone formed by a rise in the solidus temperatures on the order of 25 to 50°C. The crystallization of the pegmatite through the third intermediate zone may well have taken place over a narrow temperature interval. The solidus may have been less than 600°C owing to the high B content (Pichavant, 1981) and perhaps even lower because of the combined effects of H_2O, B, F, and Li (Manning et al., 1984). Once the pegmatite began to crystallize and volatiles were gradually removed from the system, crystallization may have proceeded under the influence of only a slight temperature gradient.

Tourmaline of the pegmatite core (types 9 and 10) is Mg depleted and ranges in Fe content from 0.5 atoms per formula unit to below the detection limit of the microprobe (Fig. 16e). The two distinct varieties of tourmaline of the core may reflect both crystallization from the residual melt and the presence of the last portion of exsolved aqueous fluid. The light-bluish-gray tourmaline (type 9), which occurs in a fine-grained intergrowth of quartz, cleavelandite, and lepidolite, may result from crystallization of the last portion of residual melt. This tourmaline is embayed and crosscut by the other minerals; therefore, it formed early in the crystallization of the core. The lack of a continuum in Mg and Fe contents from third-intermediate-zone tourmaline to core tourmaline may result from a sampling gap, or it may reflect a dilution of these elements due to their uptake by lepidolite as well as by tourmaline (Table 6).

Pink elbaite (type 10) is the most highly evolved tourmaline in the pegmatite in terms of Li enrichment and Fe depletion. The commonly euhedral form and splayed habit, and the apparent preferential occurrence of this tourmaline with small quartz segregations (Norton, 1983), may reflect crystallization in the presence of the latest-exsolved aqueous fluid. F depletion in type 10 relative to type 9 tourmaline may also indicate crystallization of type 10 in the presence of an aqueous fluid; however, dilution of F by incorporation in lepidolite is also possible. The distributions of the minor elements (Mn, Zn, Ti, Ca) between types 9 and 10 tourmaline are not easily interpreted in terms of differentiation between the aqueous and magmatic phases. Manganese is most concentrated in type 10 tourmaline, and the Zn concentration decreases relative to type 9 tourmaline. This may result from the crystal-chemical preference of the tourmaline structure. If, however, Mn and Zn are depleted in the residual melt because of preferential partitioning into the coexisting aqueous phase, why are they not depleted in tourmaline that is inferred to have crystallized from the residual melt (type 9)? The partition coefficients based on a simple Cl-rich system may be an order of magnitude too high for an F-rich system, owing to the complexing effect of F (Manning, 1981). Although Mn and Zn can be effectively fractionated between the aqueous phase and silicate melt by Cl complexing, they may not be completely removed from the melt (in an F-rich system), as might occur in a Cl-rich system. It may therefore be possible for Mn and Zn to persist in the residual melt. The reason that the two distinct tourmaline types (9 and 10) follow the same trends (Fe and Zn depletion; Li, Mn, and Ca enrichment) may be that Cl was depleted and F dominant during core formation, and therefore the crystal-chemical behavior (site preference) of tourmaline was not overprinted by a strong fractionation of elements between the melt and aqueous fluid.

The reason for the increase in Ca concentration of tourmaline throughout the pegmatite, for samples with relatively low total (Fe + Mg), is not certain; however, this trend was also noted by Staatz et al. (1955) and Foord (1976). Staatz et al. suggested that this might be a crystal-

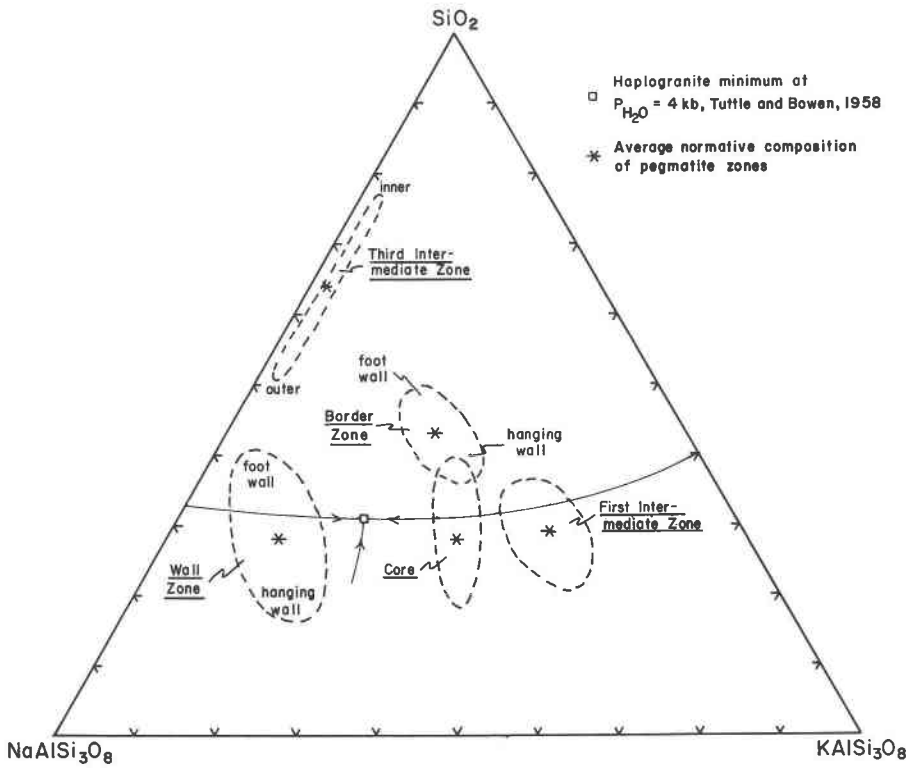

Fig. 20. Plot of approximate compositions of pegmatite zones normalized to 100 wt% quartz-albite-orthoclase. Minimum at 4 kbar in Qz-Ab-Or-H_2O haplogranite system (Tuttle and Bowen, 1958) shown for reference. Dashed circles show general trends of estimated bulk compositional variations of pegmatite zones.

chemical response, driven by charge-balance requirements of the tourmaline. The occurrence of the Ca buildup in high-Li tourmaline regardless of zonal location or textural type supports this suggestion. Another possible cause is the continuous subsolidus release of Ca from early-formed plagioclase as it equilibrates with progressively more-evolved, lower-temperature fluids (Jahns, 1982). The observed increase in Ca content of apatite from the wall zone to the core at the Bob Ingersoll No. 1 dike (Papike et al., 1984) and the occurrence of microlite, a Ca-Na tantalum oxide, in the pegmatite core support this possibility. Additionally, London and Burt (1982a) have noted postmagmatic Ca-for-Li and Ca-for-Mn exchange in primary phosphates. An actual increase in the activity of Ca is favored over the charge-balance argument as the cause of increasing Ca in late tourmaline because the most Ca-enriched tourmaline contains Al(Y) in excess of Li, a condition that does not appear to require excess positive charge for balance.

Sequence of crystallization of pegmatite zones and internal evolution

Textures observed at the Bob Ingersoll No. 1 dike coupled with compositional data on tourmaline provide insight to the sequence of crystallization of the pegmatite zones and possibly to mechanisms that were in part responsible for the compositional differentiation of the pegmatite. One possible model into which the data can be integrated with current thinking (esp. Jahns, 1982) regarding pegmatite internal evolution is described below.

The early stages of crystallization during or immediately following emplacement of the pegmatite consisted of an initial B metasomatism of the country rock and the formation of the border zone. The initial solidus temperature may have been depressed to well below 600°C on the basis of the H_2O, Li, B, and F enrichment of the pegmatite (Chorlton and Martin, 1978; Stewart, 1978; Manning, 1981; Pichavant, 1981; Manning et al., 1984). The fine-grained border zone may represent a "quench" due to volatile loss (causing an abrupt increase in the solidus). The border zone is silica rich (Fig. 20) relative to the haplogranite minimum and is also peraluminous. The peraluminous nature may only be apparent, resulting from a loss of alkalis, especially K, to the country rock (Norton, 1983). Alkali loss has been documented for many Black Hills pegmatites (e.g., Sheridan et al., 1957; Redden, 1963; Shearer et al., 1986) and specifically for the Bob Ingersoll pegmatite (Tuzinski, 1983). Zoned tourmaline crystals in the border zone may reflect enrichments and depletions caused by initial pulses of exsolving aqueous fluids. The

Mg content of the border-zone tourmaline probably results from trace Mg in the melt and from contamination by country rock.

In the wall zone, the presence of large tourmaline crystals that are perpendicular to and tapered toward the border zone indicates unobstructed crystallization from the border inward. The coarse grain size provides evidence for the presence of exsolved aqueous fluid (Jahns and Burnham, 1969). The aqueous fluid may have existed initially along growing-crystal boundaries or as fine, dispersed droplets in the melt (Jahns, 1982). The composition of tourmaline in the outer wall zone reflects the presence of the aqueous fluid in terms of the efficient, systematic differentiation of Fe, Mg, Mn, Zn, and F.

Tourmaline paragenesis, based upon the extent of the substitution of (Li + Al) for (Fe + Mg), suggests overlap in the timing of crystallization of the interior part of the wall zone, the first intermediate zone, and the third intermediate zone. The crystallization of these three zones may be complementary. The first intermediate zone is greatly enriched in K, based on the modal abundance of K-feldspar, whereas the third intermediate zone and much of the interior of the wall zone are depleted of K. Whether the reason for this differentiation lies with the response to a temperature gradient or with melt-site preference for Na relative to K, the first intermediate zone, which formed a broad thick hood in the upper portion of the pegmatite, was greatly enriched in K, a typical feature in Black Hills pegmatites (Norton and others, 1964). Transport in a fluid phase that rises through the melt because of its lower density is an appealing mechanism to achieve such differentiation. Although K may also have been depleted from the top of the pegmatite by the exsolving aqueous fluid that moved upward into the country rock, it was replenished from lower zones. The K-feldspar-bearing zone therefore crystallized with a bulk composition far removed from the quartz–K-feldspar–albite minimum toward the K-feldspar–quartz sideline (Fig. 20) or toward the K-feldspar apex. The effect of wholesale removal of K from lower parts of the pegmatite is to displace the composition of the rest magma from the ternary minimum toward the quartz-albite join, or locally even into the quartz or albite single-phase fields, but not far from the minimum, on the basis of the presence of minor amounts of muscovite or K-feldspar in the inner wall zone and third intermediate zone. Additionally, the displacement from the minimum composition should result in forced crystallization of quartz and albite (Jahns, 1982).

As the composition of the residual melt moved away from the minimum composition, its ability to retain water in solution, in terms of weight percent, may have increased (Fig. 27, Tuttle and Bowen, 1958). Alternatively, the lack of tourmaline crystallization in outer parts of the third intermediate zone allowed the component $Li_2B_4O_7$ (or other alkali borate) to concentrate in the residual melt, causing increased H_2O–silicate liquid miscibility as shown by London (1986). The significance of these compositional shifts is that the magma forming the third intermediate zone was forced to at least partially crystallize and that there may have been a hiatus in the aqueous-fluid exsolution. Tourmaline of this zone does not show the compositional or textural characteristics that are inferred to result from coexistence with an aqueous-fluid component with the melt. Tourmaline eventually became stable and resumed crystallization. Removal of $Li_2B_4O_7$ from the melt caused H_2O exsolution to resume, which in turn caused increased melt polymerization and deposition of beryl, apatite, and cassiterite. Another important compositional aspect of the third intermediate zone is the abundance of quartz (relative to cleavelandite), which appears to increase gradually, beginning in cleavelandite-rich portions of the wall zone. The increase in modal quartz is also consistent with the possibility that the third intermediate zone is a product of a residual magma. As such, it should be enriched in F, and this is indeed indicated by the high F content of third-intermediate-zone tourmaline. An increase in F concentration in the silicate melt has the effect of shifting the quartz-albite join away from the quartz apex (Manning, 1981), thus causing an increasing proportion of quartz crystallization.

As a consequence of pegmatite crystallization, the activity of Li in the residual silicate melt increases (Stewart, 1978). Eventually, with the continued crystallization of quartz and alkali feldspars, the composition of the residual silicate melt reaches a minimum in the quartz–alkali feldspar–eucryptite ($LiAlSiO_4$) ternary system (Fig. 21), and one of the lithium aluminosilicates begins to crystallize. At the Bob Ingersoll No. 1 dike, the primary Li mineral that formed is lepidolite, probably owing to the abundance of F (London and Burt, 1982b; Černý and Burt, 1984). This zone (quartz-cleavelandite-lepidolite) forms the structural center of the dike and is inferred to be the core in the sense that it was last to crystallize, on the basis of the occurrence of highly evolved, primary tourmaline.

Conclusions

Tourmaline from the internally zoned Bob Ingersoll No. 1 pegmatite dike occurs as a number of texturally and compositionally distinct types that are confined to particular zones. The tourmaline compositions are mostly along the schorl-elbaite join, ranging from slightly over 50% of the schorl end member to nearly end-member elbaite. Several of the groups contain appreciable Mg; Zn, Mn, Ti, and Ca are minor constituents. Tourmaline exhibits systematic compositional variations that indicate B metasomatism of the country rock, followed by the progressive crystallization of the pegmatite in the sequence border zone to wall zone to intermediate zones to core. The major substitution corresponding to progressive evolution of the pegmatite is (Li + Al) replacing (Fe^{2+} + Mg) in the Y site. This is generally consistent with the findings of other studies. However, variations in minor-element concentrations suggest that a complex crystallization relationship exists among the intermediate zones of the pegmatite.

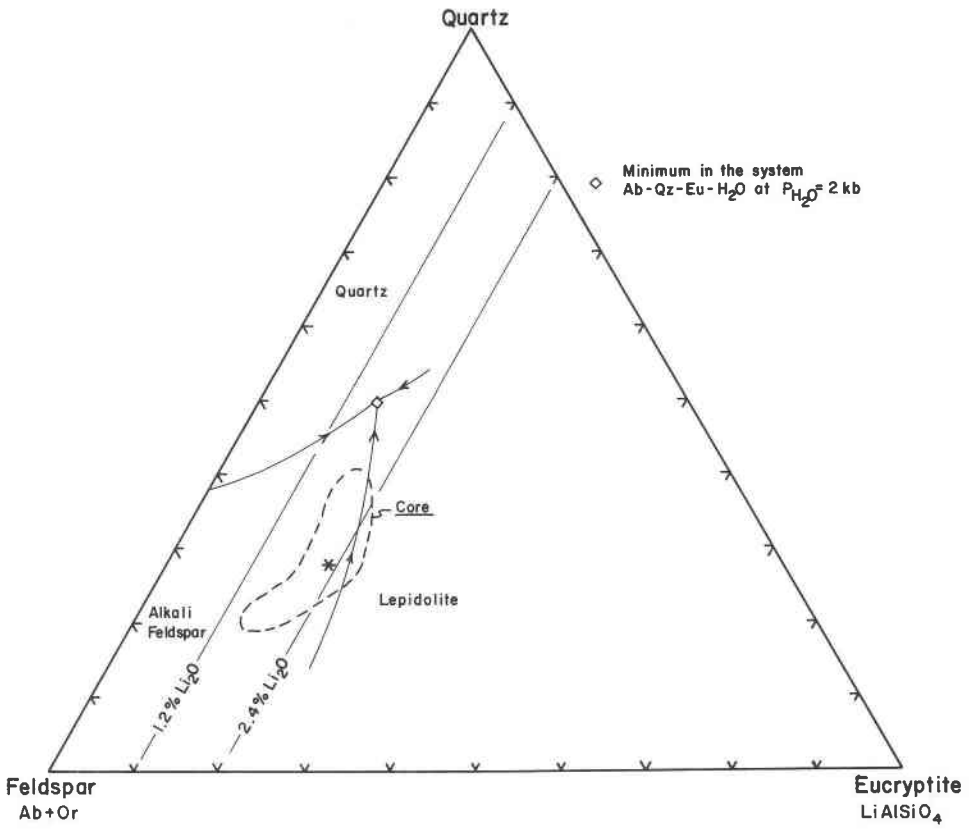

Fig. 21. Plot of composition of pegmatite core, normalized to 100 wt% combined alkali feldspars, quartz, and eucryptite (after Stewart, 1978). Minimum of the system Ab-Qz-eucryptite-H_2O at P_{H_2O} = 2 kbar and approximate field boundaries for Li minerals in general (Stewart, 1978) shown for reference.

Interpretations regarding the nature of crystallization relationships of the zones and the nature of crystallization medium depend upon the recognition of three factors that affect the compositional variation of tourmaline: (1) bulk compositional evolution of the pegmatite melt-fluid system during progressive crystallization; (2) the crystallization process, particularly the nature of the crystallizing medium; and (3) crystal-chemical preferences of the tourmaline structure in response to changing physical conditions. Regarding the second factor, three processes are of concern: metasomatism, crystallization from a silicate melt, and crystallization from a silicate melt in the presence of an exsolving aqueous fluid. Of particular importance is the differentiation capability of the separate aqueous fluid, whether in a "static" sense or in the sense of a mobile fluid that differentially scavenges elements from one portion of the melt and enriches the melt elsewhere. By distinguishing the effects of these factors, compositional variations of the tourmaline may be useful in the interpretation of crystallization processes that affected the differentiation of a given pegmatite.

Textures and crystal-zoning trends support the compositional trends and are consistent with the following model for the Bob Ingersoll No. 1 pegmatite. The border zone crystallized as a quenched margin owing to volatile loss during an initial pulse of exsolving fluid synchronously with B metasomatism and formation of tourmaline in the country rock. The pegmatite initially crystallized from the walls inward and exsolved aqueous fluid throughout wall-zone crystallization. The aqueous fluid provided an effective medium for differentiating the pegmatite melt with respect to several constituents, including the Y-site cations of tourmaline and the alkalis Na and K. As the aqueous fluid concentrated in upper parts of the pegmatite, K became enriched and formed the K-feldspar-rich first intermediate zone. The depletion of K resulted in the increasingly sodic nature of the inner wall zone and the adjacent third intermediate (quartz-cleavelandite) zone in lower parts of the dike. The suppression of tourmaline crystallization coupled with the depletion of K in the third intermediate zone changed the bulk composition of the rest magma, and crystallization of the quartz-cleavelandite zone occurred without concomitant exsolution of aqueous fluid. When conditions again became favorable, tourmaline crystallization resumed, depleted the melt in Li and B fluxing components, and contributed toward renewed exsolution of aqueous fluid. The rest magma achieved Li saturation and crystallized a min-

imum-melt assemblage of quartz-cleavelandite-lepidolite at the core of the pegmatite, which also contains the most-evolved tourmaline, Fe-free elbaite.

Many of the interpretations presented in this study are speculative. Research in several specific areas may provide additional insights. These include the stability of tourmaline and its equilibrium composition, in terms of major end members, under diverse conditions. Data pertaining to the partitioning behavior of elements in the system melt-fluid-crystals, with different combined concentrations of the elements F, Cl, and B, are also critical to improved understanding of chemical differentiation during the internal evolution of zoned pegmatites.

Acknowledgments

We are greatly indebted to the following individuals: V. Jensen, word processing; R. Talbot, drafting; D. Gosselin and A. Settle for assistance with mapping and sampling; C. Larive, fluorine determinations; S. Simon, computer applications; W. L. Roberts for supplying sample S1; J. C. Laul and Battelle, Pacific Northwest Laboratories, INAA; B. L. Davis, X-ray diffraction patterns; and E. E. Foord for providing tourmaline samples for analytical comparison. The manuscript was greatly improved by the advice and review of J. A. Redden, E. E. Foord, D. London, R. V. Dietrich, P. J. Dunn, J. J. Norton, and R. J. Walker. This work was supported by the National Science Foundation under NSF Graduate Fellowship RCD-8450127 (B. L. Jolliff) and by the U.S. Department of Energy under DOE grant DE-FG01-84ER13259 (J. J. Papike).

References

Barton, R., Jr. (1969) Refinement of the crystal structure of buergerite and the absolute orientation of tourmalines. Acta Crystallographica, B25, 1525–1533.

Bence, A.E., and Albee, A.L. (1968) Empirical correction factors for the electron microanalysis of silicates and oxides. Journal of Geology, 76, 382–403.

Bloss, F.D. (1971) Crystallography and crystal chemistry. Holt, Rhinehart and Winston, New York.

Bodkin, J.B. (1977) Determination of fluorine by use of an ion-selective electrode following fusion with lithium metaborate. The Analyst, 102, 409–413.

Bradley, J.E.S., and Bradley, O. (1953) Observations on the coloring of pink and green zoned tourmaline. Mineralogical Magazine, 30, 26–38.

Buerger, M.J., Burnham, C.W., and Peacor, D.R. (1962) Assessment of several structures proposed for tourmaline. Acta Crystallographica, 15, 583–590.

Burnham, C.W. (1979) Magmas and hydrothermal fluids. In H.L. Barnes, Ed. Geochemistry of hydrothermal ore deposits, 71–136. Wiley, New York.

Carobbi, G., and Pieruccini, R. (1947) Spectrographic analysis of tourmalines from the Island of Elba with correlation of color and composition. American Mineralogist, 32, 121–130.

Černý, Petr. (1975) Granitic pegmatites and their minerals: Selected examples of recent progress. Fortschritte der Mineralogie, 52, 225–250.

——— (1982) Petrogenesis of granitic pegmatites. In Petr Černý, Ed. Short course in granitic pegmatites in science and industry, 405–461. Mineralogical Association of Canada Short Course Handbook 8.

Černý, Petr, and Burt, D.M. (1984) Paragenesis, crystallochemical characteristics, and geochemical evolution of micas in pegmatites. In S.W. Bailey, Ed. Micas, 259–297. Mineralogical Society of America Reviews in Mineralogy, 13.

Chaudhry, M.N., and Howie, R.A. (1976) Lithium tourmaline from the Meldon aplite, Devonshire, England. Mineralogical Magazine, 40, 747–751.

Chorlton, L.B., and Martin, R.F. (1978) The effect of boron on the granite solidus. Canadian Mineralogist, 16, 239–244.

Deer, W.A., Howie, R.A., and Zussman, J. (1962) Rock forming minerals. Volume 1, Ortho- and ring silicates, fourth edition, 300–319. Wiley, New York.

Donnay, G. (1968) Crystalline heterogeneity: Evidence from the electron-probe study of Brazilian tourmaline. Carnegie Institution of Washington Year Book 67, 219–220.

Donnay, G., and Barton, R., Jr. (1972) Refinement of the crystal structure of elbaite and the mechanism of tourmaline solid solution. Tschermaks Mineralogische und Petrographische Mitteilungen, 18, 273–286.

Donnay, G., Ingamells, C.O., and Mason, B. (1966) Buergerite, a new species of tourmaline. American Mineralogist, 51, 198–199.

Dowty, E. (1980) Crystal growth and nucleation theory and the numerical simulation of igneous crystallization. In R.B. Hargraves, Ed. Physics of magmatic processes, 419–485. Princeton University Press, Princeton, New Jersey.

Dunn, P.J. (1977) Chromium in dravite. Mineralogical Magazine, 41, 408–410.

Dunn, P.J., Appleman, D.E., and Nelen, J.E. (1977a) Liddicoatite, a new calcium end-member of the tourmaline group. American Mineralogist, 62, 1121–1124.

Dunn, P.J., Appleman, D.E., Nelen, J.A., and Norberg, J. (1977b) Uvite, a new (old) common member of the tourmaline group and its implications to collectors. Mineralogical Record, 8, 100–108.

Ekambaram, V., Rosenberg, P.E., and Foit, F.F., Jr. (1981) Synthesis and characterization of tourmaline in the system Na_2O-Al_2O_3-SiO_2-B_2O_3-H_2O. EOS American Geophysical Union Transactions, 62, 1065.

El-Hinnawi, E.E., and Hofmann, R. (1966) Optische und chemische Untersuchungen an neun Turmalinen (Elbaiten). Neues Jahrbuch für Mineralogie, Monatshefte, 80–89.

Epprecht, W. (1953) Die Gitterkonstanten der Turmaline. Schweizerische Mineralogische und Petrographische Mitteilungen, 33, 481–505.

Faye, G.H., Manning, P.G., Gosselin, J.R., and Tremblay, R.J. (1974) The optical absorption spectra of tourmaline: Importance of charge-transfer processes. Canadian Mineralogist, 12, 370–380.

Foit, F.F., Jr., and Rosenberg, P.E. (1977) Coupled substitutions in the tourmaline group. Contributions to Mineralogy and Petrology, 62, 109–127.

——— (1979) The structure of vanadium-bearing tourmaline and its implications regarding tourmaline solid solutions. American Mineralogist, 64, 788–798.

Foord, E.E. (1976) Mineralogy and petrogenesis of layered pegmatite-aplite dikes in the Mesa Grande District, San Diego County, California. Ph.D. thesis, Stanford University, Stanford, California.

——— (1977) The Himalaya dike system, Mesa Grande district, San Diego County, California. Mineralogical Record, 8, 461–474.

Fortier, S., and Donnay, G. (1975) Schorl refinement showing compositional dependence of the tourmaline structure. Canadian Mineralogist, 13, 173–177.

Frondel, C., Biedl, A., and Ito, J. (1966) New type of ferric iron tourmaline. American Mineralogist, 51, 1501–1505.

Fuge, R. (1977) On the behavior of fluorine and chlorine during magmatic differentiation. Contributions to Mineralogy and Petrology, 61, 245–249.

Hanley, J. B. (1953) Bob Ingersoll mine (Keystone district). In L.R. Page and others, Pegmatite investigations, 1942–1945,

Black Hills, South Dakota. U.S. Geological Survey Professional Paper 247, 75–78.

Hards, N. (1976) Distribution of elements between the fluid phase and silicate melt phase of granites and nepheline syenites. In Progress in experimental petrology. Natural Environment Research Council Report D6, 88–90.

Henry, D.J., and Guidotti, C.V. (1985) Tourmaline as a petrogenetic indicator mineral: An example from the staurolite-grade metapelites of NW Maine. American Mineralogist, 70, 1–15.

Hermon, E., Simkin, D.J., Donnay, G., and Muir, W.B. (1972) The distribution of Fe^{2+} and Fe^{3+} in iron-bearing tourmalines: A Mössbauer study. Tschermaks Mineralogische und Petrographische Mitteilungen, 19, 124–132.

Holland, H.D. (1972) Granites, solutions, and base metal deposits. Economic Geology, 67, 281–301.

Ito, T., and Sadanaga, R. (1951) A Fourier analysis of the structure of tourmaline. Acta Crystallographica, 4, 385–390.

Jahns, R.H. (1953) The genesis of pegmatites I. Occurrence and origin of giant crystals. American Mineralogist, 38, 563–598.

——— (1955) The study of pegmatites. Economic Geology, Fiftieth Anniversary Volume, Part II, 1023–1130.

——— (1982) Internal evolution of pegmatite bodies. In Petr Černý, Ed. Granitic pegmatites in science and industry, 293–327. Mineralogical Association of Canada Short Course Handbook 8.

Jahns, R.H., and Burnham, C.W. (1969) Experimental studies of pegmatite genesis: I. A model for the derivation and crystallization of granitic pegmatites. Economic Geology, 64, 843–864.

Jenks, W.F. (1935) Pegmatites at Collins Hill, Portland, Connecticut. American Journal of Science, 5th series, 30, 177–197.

Jensen, M. (1984) Major, minor, and trace elements (REE's) in apatite as recorders of pegmatite petrogensis. M.S. thesis, South Dakota School of Mines and Technology, Rapid City.

Laul, J.C. (1979) Neutron activation analysis of geological materials. Review article for Atomic Energy Review, IAEA, 17, No. 3, 603–697.

Leckebusch, R. (1978) Chemical composition and color of tourmalines from Darre Pech (Nuristan, Afghanistan). Neues Jahrbuch für Mineralogie Abhandlungen, 133, 53–70.

Lofgren, G. (1980) Experimental studies on the dynamic crystallization of silicate melts. In R.B. Hargraves, Ed. Physics of magmatic processes, 487–551. Princeton University Press, Princeton, New Jersey.

London, D. (1986) Magmatic-hydrothermal transition in the Tanco rare-element pegmatite: Evidence from fluid inclusions and phase-equilibrium experiments. American Mineralogist, 71, 376–395.

London, D., and Burt, D.M. (1982a) Alteration of spodumene, montebrasite and lithiophilite in pegmatites of the White Picacho District, Arizona. American Mineralogist, 67, 97–113.

——— (1982b) Lithium minerals in pegmatites. In Petr Černý, Ed. Granitic pegmatites in science and industry, 99–133. Mineralogical Association of Canada Short Course Handbook 8.

Manning, D.A.C. (1981) The effect of fluorine on liquidus phase relationships in the system Qz-Ab-Or with excess water at 1 Kb. Contributions to Mineralogy and Petrology, 76, 206–215.

——— (1982) Chemical and morphological variation in tourmalines from the Hub Kapong batholith of peninsular Thailand. Mineralogical Magazine, 45, 139–147.

Manning, D.A.C., Martin, J.S., Pichavant, M., and Henderson, C.M.B. (1984) The effect of F, B and Li on melt structures in the granite system: different mechanisms? In Progress in experimental petrology, 36–41. Natural Environment Research Council Report D25.

Moore, J.G., and Lockwood, J.P. (1973) Origin of comb layering and orbicular structure, Sierra Nevada batholith, California. Geological Society of America Bulletin, 84, 1–20.

Moore, P.B. (1982) Pegmatite minerals of P(V) and B(III). In Petr Černý, Ed. Granitic pegmatites in science and industry, 267–291. Mineralogical Association of Canada Short Course Handbook 8.

Neiva, A.M.R. (1974) Geochemistry of tourmaline (schorlite) from granites, aplites and pegmatites from Northern Portugal. Geochimica et Cosmochimica Acta, 38, 1307–1317.

Nemec, D. (1969) Fluorine in tourmalines. Contributions to Mineralogy and Petrology, 20, 235–243.

Norton, J.J. (1983) Sequence of mineral assemblages in differentiated granitic pegmatites. Economic Geology, 78, 854–874.

Norton, J.J., Page, L.R., and Brobst, D.A. (1962) Geology of the Hugo pegmatite, Keystone, South Dakota. U.S. Geological Survey Professional Paper 297-B, 49–127.

Norton, J.J., and others (1964) Geology and mineral deposits of some pegmatites in the southern Black Hills, South Dakota. U.S. Geological Survey Professional Paper 297-E, 293–341.

Nuber, B., and Schmetzer, K. (1979) The lattice position of Cr^{3+} in tourmaline: Structural refinement of a chromium-rich Mg-Al-tourmaline. Neues Jahrbuch für Mineralogie Abhandlungen, 184–197.

——— (1981) Strukturverfeinerung von Liddicoatit. Neues Jahrbuch für Mineralogie, Monatshefte, 215–219.

Page, L.R., and others (1953) Pegmatite investigations 1942–1945, Black Hills, South Dakota. U.S. Geological Survey Professional Paper 247.

Papike, J.J., Jensen, M., Shearer, C.K., Simon, S.B., Jolliff, B.L., Walker, R.J., and Laul, J.C. (1984) Apatite as a recorder of pegmatite petrogenesis. Geological Society of America Abstracts with Programs, 16, 617.

Pichavant, M. (1981) An experimental study of the effect of boron on a water saturated haplogranite at 1 Kbar vapour pressure. Contributions to Mineralogy and Petrology, 76, 430–439.

Power, G.M. (1968) Chemical variation in tourmalines from southwest England. Mineralogical Magazine, 36, 1078–1098.

Redden, J.A. (1963) Geology and pegmatites of the Fourmile quadrangle, Black Hills, South Dakota. U.S. Geological Survey Professional Paper 297-D, 199–291.

Redden, J.A., Norton, J.J., and McLaughlin, R.J. (1982) Geology of the Harney Peak Granite. U.S. Geological Survey Open-File Report 82-481.

Roberts, W.L., and Rapp, G., Jr. (1965) Mineralogy of the Black Hills, Bulletin Number 18, South Dakota School of Mines and Technology, Rapid City, South Dakota.

Roegge, J.S., Logsdon, M.J., Young, H.S., Barr, H.B., Borcsik, M., and Holland, H.D. (1974) Halogens in apatites from the Providencia Area, Mexico. Economic Geology, 69, 229–240.

Rose, D., Langer, K., and Tennyson, CH. (1981) Turmalin Farbe und Paragenese. Fortschritte der Mineralogie, 59, 164–166.

Rosenberg, P.E., and Foit, F.F., Jr. (1979) Synthesis and characterization of alkali free tourmaline. American Mineralogist, 64, 180–186.

Rumantseva, E.V. (1983) Chromdravite, a new mineral. Zapiski Vsesoyuznogo Mineralogicheskogo Obshchestva, 112, 222–226. (English summary in American Mineralogist, 69, 210.)

Sahama, Th.G., v. Knorring, O., and Törnroos, R. (1979) On tourmaline. Lithos, 12, 109–114.

Schmetzer, K., and Bank, H. (1984) Crystal chemistry of tsilaisite (manganese tourmaline) from Zambia. Neues Jahrbuch für Mineralogie, Monatshefte, 61–69.

Schmetzer, K., Nuber, B., and Abraham, K. (1979) Crystal chemistry of magnesium-rich tourmalines. Neues Jahrbuch für Mineralogie Abhandlungen, 136, 93–112.

Shearer, C.K., Papike, J.J., and Laul, J.C. (1985) Chemistry of potassium feldspars from three zoned pegmatites, Black Hills, South Dakota: Implications concerning pegmatite evolution. Geochimica et Cosmochimica Acta, 49, 663–673.

Shearer, C.K., Papike, J.J., Simon, S.B., and Laul, J.C. (1986) Pegmatite/wallrock interactions, Black Hills, South Dakota: Interaction between pegmatite-derived fluids and quartz-mica schist wallrock. American Mineralogist, 71, 518–539.

Sheridan, D.M., Stephens, H.G., Staatz, M.H., and Norton, J.J. (1957) Geology and beryl deposits of the Peerless pegmatite, Pennington County, South Dakota. U.S. Geological Survey Professional Paper 297-A, 1–47.

Slivko, M.M. (1965) On inclusions of solutions in crystals of tourmaline. In E. Roedder, Ed. Research on the nature of mineral-forming solutions. International Series of Monographs in Earth Science, 22, Part III, 626–634.

Snetsinger, K.G. (1966) Barium-vanadium muscovite and vanadium tourmaline from Mariposa County, California. American Mineralogist, 51, 1623–1639.

Staatz, M.H., Murata, K.J., and Glass, J. J. (1955) Variation of composition and physical properties of tourmaline with its position in the pegmatite. American Mineralogist, 40, 789–804.

Stewart, D.B. (1978) Petrogenesis of lithium-rich pegmatites. American Mineralogist, 63, 970–980.

Tauson, L.V. (1965) Factors in the distribution of the trace elements during the crystallization of magmas. Physics and Chemistry of the Earth, 6, 215–249.

Taylor, A.M., and Terrell, B.C. (1967) Synthetic tourmalines containing elements of the first transition series. Journal of Crystal Growth, 1, 238–244.

Tuttle, O.F., and Bowen, N.L. (1958) Origin of granite in the light of experimental studies in the system $NaAlSi_3O_8$-$KAlSi_3O_8$-SiO_2-H_2O. Geological Society of America Memoir 74.

Tuzinski, P.A. (1983) Rare-alkali ion halos surrounding the Bob Ingersoll lithium-bearing pegmatite mine, Keystone, Black Hills, South Dakota. M.S. thesis, Kent State University, Kent, Ohio.

Walenta, K., and Dunn, P.J. (1979) Ferridravite, a new mineral of the tourmaline group from Bolivia. American Mineralogist, 64, 945–949.

Werding, G., and Schreyer, W. (1984) Alkali-free tourmaline in the system MgO-Al_2O_3-B_2O_3-SiO_2-H_2O. Geochimica et Cosmochimica Acta, 48, 1331–1344.

Wilkins, R.W.T., Farrell, E.F., and Naiman, C.S. (1969) The crystal field spectra and dichroism of tourmaline. Journal of Physics and Chemistry of Solids, 30, 43–56.

Zoltai, T., and Stout, J.H. (1984) Mineralogy, concepts and principles, 135–183. Burgess Publishing Company, Minneapolis.

Manuscript received February 28, 1985
Manuscript accepted November 11, 1985